

AD-A031 777

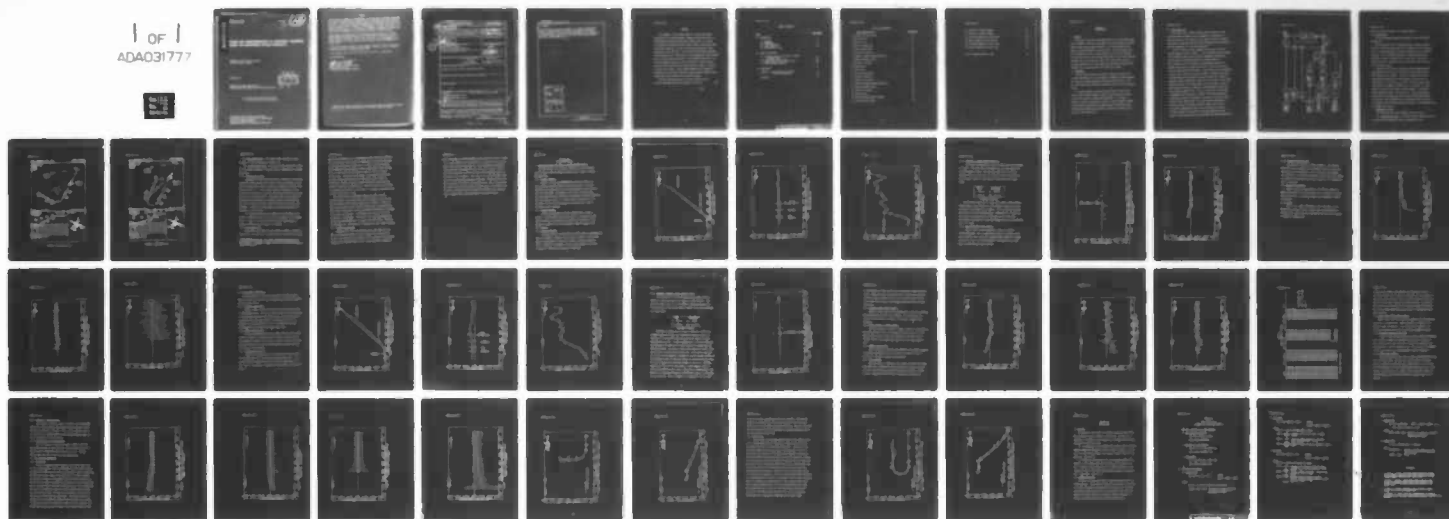
AIR FORCE FLIGHT DYNAMICS LAB WRIGHT-PATTERSON AFB OHIO F/G 1/4
FLIGHT TEST DEMONSTRATION OF AUTOMATIC LANDINGS BASED ON MICROW--ETC(U)
AUG 76 D EASTMAN, P CLOUGH

UNCLASSIFIED

AFFDL-TR-76-105

NL

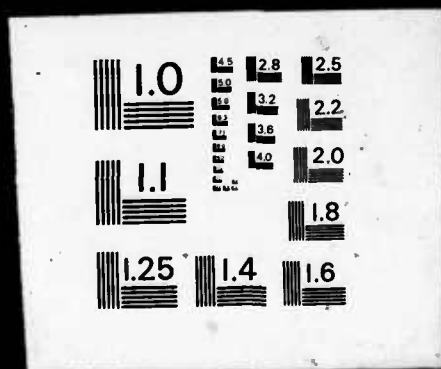
1 OF 1
ADA031777



END

DATE
FILMED
12 - 76

1 OF 1
ADA031777



ADA031777

AFFDL-TR-76-105

12

FLIGHT TEST DEMONSTRATION OF AUTOMATIC LANDINGS BASED ON MICROWAVE SYSTEM GUIDANCE

TERMINAL AREA CONTROL BRANCH
FLIGHT CONTROL DIVISION

AUGUST 1976

TECHNICAL REPORT AFFDL-TR-76-105
FINAL REPORT FOR PERIOD MARCH THROUGH MAY 1976

D D C
RECEIVED
NOV 9 1976
B

Approved for public release; distribution unlimited

AIR FORCE FLIGHT DYNAMICS LABORATORY
AIR FORCE WRIGHT AERONAUTICAL LABORATORIES
AIR FORCE SYSTEMS COMMAND
WRIGHT-PATTERSON AIR FORCE BASE, OHIO 45433

NOTICE

When Government drawings, specifications, or other data are used for any purpose other than in connection with a definitely related Government procurement operation, the United States Government thereby incurs no responsibility nor any obligation whatsoever; and the fact that the government may have formulated, furnished, or in any way supplied the said drawings, specifications, or other data, is not to be regarded by implication or otherwise as in any manner licensing the holder or any other person or corporation, or conveying any rights or permission to manufacture, use, or sell any patented invention that may in any way be related thereto.

This report was prepared by the Special Projects Group, Terminal Area Control Branch, Flight Control Division, Air Force Flight Dynamics Laboratory, Air Force Systems Command, Wright-Patterson Air Force Base, Ohio. The Air Force Flight Dynamics Laboratory Program Manager was Mr. Terry Emerson; Mr. Don Eastman was the Project Engineer; Mr. Jack Barry was the Test Director; and Major Joe Havas was Project Pilot.

This report has been reviewed by the Information Office (OI) and is releasable to the National Technical Information Service (NTIS). At NTIS, it will be available to the general public, including foreign nations.

This technical report has been reviewed and is approved for publication.

FOR THE COMMANDER:


EDWARD L. HEFT, Lt Col USAF
Chief, Terminal Area Control Branch
Flight Control Division
Air Force Flight Dynamics Laboratory

Copies of this report should not be returned unless return is required by security considerations, contractual obligations, or notice on a specific document.

UNCLASSIFIED

SECURITY CLASSIFICATION OF THIS PAGE (When Data Entered)

REPORT DOCUMENTATION PAGE		READ INSTRUCTIONS BEFORE COMPLETING FORM
1. AFFDL-TR-76-105	2. GOVT ACCESSION NO.	3. RECIPIENT'S CATALOG NUMBER
4. TITLE (and Subtitle) Flight Test Demonstration of Automatic Landings Based on Microwave Landing System Guidance.	5. TYPE OF REPORT AND PERIOD COVERED Final report. March - May 1976	
6. AUTHOR(s) H. Eastman P. Clough	7. PERFORMING ORG. REPORT NUMBER	
8. PERFORMING ORGANIZATION NAME AND ADDRESS Special Projects Group Terminal Area Control Branch Air Force Flight Dynamics Laboratory	9. CONTRACT OR GRANT NUMBER(s)	
10. CONTROLLING OFFICE NAME AND ADDRESS	11. PROGRAM ELEMENT, PROJECT, TASK AREA & WORK UNIT NUMBERS 404L0119	
12. MONITORING AGENCY NAME & ADDRESS (if different from Controlling Office)	13. REPORT DATE August 1976	
14. DISTRIBUTION STATEMENT (of this Report) Approval for public release; distribution unlimited.	15. NUMBER OF PAGES 67	
16. DISTRIBUTION STATEMENT (of the abstract entered in Block 20, if different from Report)	17. SECURITY CLASS. (of this report) UNCLASSIFIED	
18. SUPPLEMENTARY NOTES	19. DECLASSIFICATION/DOWNGRADING SCHEDULE	
19. KEY WORDS (Continue on reverse side if necessary and identify by block number) Landing Time Reference Scanning Beam (TRSB) Digital Flight Control Systems Complex Approach Path Microwave Landing System (MLS) Flight Test		
20. ABSTRACT (Continue on reverse side if necessary and identify by block number) This report describes the USAF participation in the gathering of data for the United States submission to The International Civil Aviation Organization of a "Non-Visual Precision Approach and Landing System for International Aviation." The report contains data on Time Referenced Scanning Beam Microwave Landing System accuracy, as recorded on the test aircraft during automatic approaches and landings. The report contains information on aircraft performance and		

DD FORM 1 JAN 73 1473

EDITION OF 1 NOV 65 IS OBSOLETE

UNCLASSIFIED

SECURITY CLASSIFICATION OF THIS PAGE (When Data Entered)

012070

02

UNCLASSIFIED

SECURITY CLASSIFICATION OF THIS PAGE(When Data Entered)

20. ABSTRACT

pilot acceptance for performing automatic MLS instrument approaches and landings. The USAF modified T-39 aircraft was capable of flying fully coupled and automatic curved and segmented approaches through landing using TRSB MLS data. The purpose of the flight testing was to demonstrate an inherent TRSB MLS capability rather than to provide a great amount of MLS accuracy or performance data.

ACCESSION by	
NTIS	White Section <input checked="" type="checkbox"/>
DDC	Buff Section <input type="checkbox"/>
UNANNOUNCED	<input type="checkbox"/>
JUSTIFICATION	
BY	
DISTRIBUTION/AVAILABILITY CODES	
Dist.	AVAIL. and/or SPECIAL
A	

UNCLASSIFIED

SECURITY CLASSIFICATION OF THIS PAGE(When Data Entered)

FOREWORD

This document is the technical report on a flight test program demonstrating fully coupled automatic landings using guidance from the Time Referenced Scanning Beam Microwave Landing System. The program was conducted by the Special Projects Group, Terminal Area Control Branch, Flight Control Division, Air Force Flight Dynamics Laboratory, Wright-Patterson Air Force Base, Ohio. The Air Force Flight Dynamics Laboratory Program Manager was Mr. Terry Emerson; Mr. Don Eastman was Project Engineer and Mr. Jack Barry was Test Director. The Instrument Flight Center, Air Training Command provided the aircraft and aircrews. Major Joe Havas was project pilot and assisted by pilot Captain's M. Rogers, J. Swenson, R. Spivey, and G. Mucho. Overall program management and funding was provided by the USAF Traffic Control and Landing Systems, TRACALS, System Program Office and the Federal Aviation Administration.

The effort described here was initiated in March 1976 and a technical memorandum TM-76-54 was submitted in May 1976.

Whi under AFFDL

X

TABLE OF CONTENTS

<u>TITLE</u>	<u>PAGE NUMBER</u>
1.0 INTRODUCTION	
1.1 Purpose	1
1.2 Background	1
1.3 Flare Control Law	2
1.4 Profile Design	4
1.5 Description of Plots	4
2.0 FLIGHT TEST RESULTS	
2.1 Elevation Antenna (EL1) Fade-In to Radio Altimeter Flare	10
2.2 Flare Antenna (EL2) Flare	21
2.3 Summary Plots of MLS Flight Accuracy	32
2.4 MLS Instrument Approaches	33
3.0 CONCLUSIONS	43
Appendix A - Data Retrieval of On-Board Data & Phototheodolite	45
References	47

TABLE OF ILLUSTRATIONS

<u>Figure Number & Title</u>	<u>Page Number</u>
1 T-39 MLS Flare Control Law	3
2 MLS Profile 231	5
3 MLS Profile 232	6
4 Vertical Tracking Plot	11
5 Lateral Tracking Plot	12
6 T-39 Vertical Velocity	13
7 Automatic Landing Touchdown Dispersion	15
8 Approach Azimuth Accuracy	16
9 Elevation 1 Accuracy	18
10 Range Accuracy	19
11 Height Error	20
12 Vertical Tracking Plot	22
13 Lateral Tracking Plot	23
14 T-39 Vertical Velocity	24
15 Automatic Landing Touchdown Dispersion	26
16 Approach Azimuth Accuracy	28
17 Elevation 2 Accuracy	29
18 Range Accuracy	30
19 Approach Azimuth Accuracy, Summary	34
20 Range Accuracy, Summary	35

APFDL-TR-76-105

21 Elevation 1 Accuracy, Summary	36
22 Elevation 2 Accuracy, Summary	37
23 Horizontal Summary Plot, Profile 231	38
24 Vertical Summary Plot, Profile 231	39
25 Horizontal Summary Plot, Profile 232	41
26 Vertical Summary Plot, Profile 232	42
 Table 1, Range Transients at GPIIP	 31

SECTION 1.0 INTRODUCTION

1.1 Purpose

The purpose of the flight test demonstration was to obtain operational data for automatic landings using guidance from the Time Reference Scanning Beam Microwave Landing System (TRSB MLS). Two techniques were used to obtain altitude information for flare guidance: (1) MLS Elevation Data (EL1) and DME were used to calculate height until the aircraft reached 50 feet above the Glide Path Intercept Point (GPIP) or near runway threshold whereupon the radio altimeter was faded in for flare control, and (2) the same derived height as above except that the height information after threshold was calculated from MLS Flare Data (EL2) and DME.

1.2 Background

Previous flight testing was conducted in August and October 1975 to obtain operational data on the adequacy of TRSB MLS to provide guidance for curved and segmented approaches (Reference AFFDL-TR-76-43). Data was taken during eight designed MLS approaches flown to a 100 foot decision height.

This report presents the data from flights flown in April 1976; these flights included automatic landings achieved after flying one of two specified curved and segmented MLS approaches. In addition to automatic straight-in approaches to landing, 20 fully automatic landings, using both flare techniques, were completed after flying MLS profiles. Both aircraft performance data and MLS error data is presented in this report for these flight tests.

1.3 Flare Control Law

Flare control laws of today, which are generally based on radio altitude derived displacement and rate commands, are susceptible to terrain variations in the proximity of the runway; therefore a technique was devised to transition from MLS derived information to radio altimeter derived information at or near runway threshold.

The MLS EL1 fade-in to radio altimeter flare control law used in the test program is shown in Figure 1. This configuration takes advantage of the benefits of MLS by using a terrain independent altitude (HEL1) derived from the EL1 angle and DME data to initiate fade-in to radio altimeter; flare is initiated at a preselected altitude using whichever data source is current at that time. As the aircraft passes over the runway threshold (1000 feet in front of GPIP) the radio altimeter altitude and its derived rate signal are faded in through the transition filter defined by $(1-F(X))$ while EL1 control is faded out. Damping is provided by normal acceleration, washed out pitch attitude and pitch rate. The MLS EL1 fade-in to EL2 flare control law is also shown in Figure 1; radio altimeter altitude is replaced with altitude (HEL2) derived from the EL2 angle and DME distance. The basic flare control law provides a programmed rate of descent as a function of the altitude reference, essentially providing an "exponential" path that is not fixed in space relative to the runway surface. The rate of descent information is derived from the flare altitude reference signal, using a normal acceleration complementary filter to reduce spurious noise effects. The rate of descent error signal is processed through the elevator control system through appropriate displacement and integral terms which

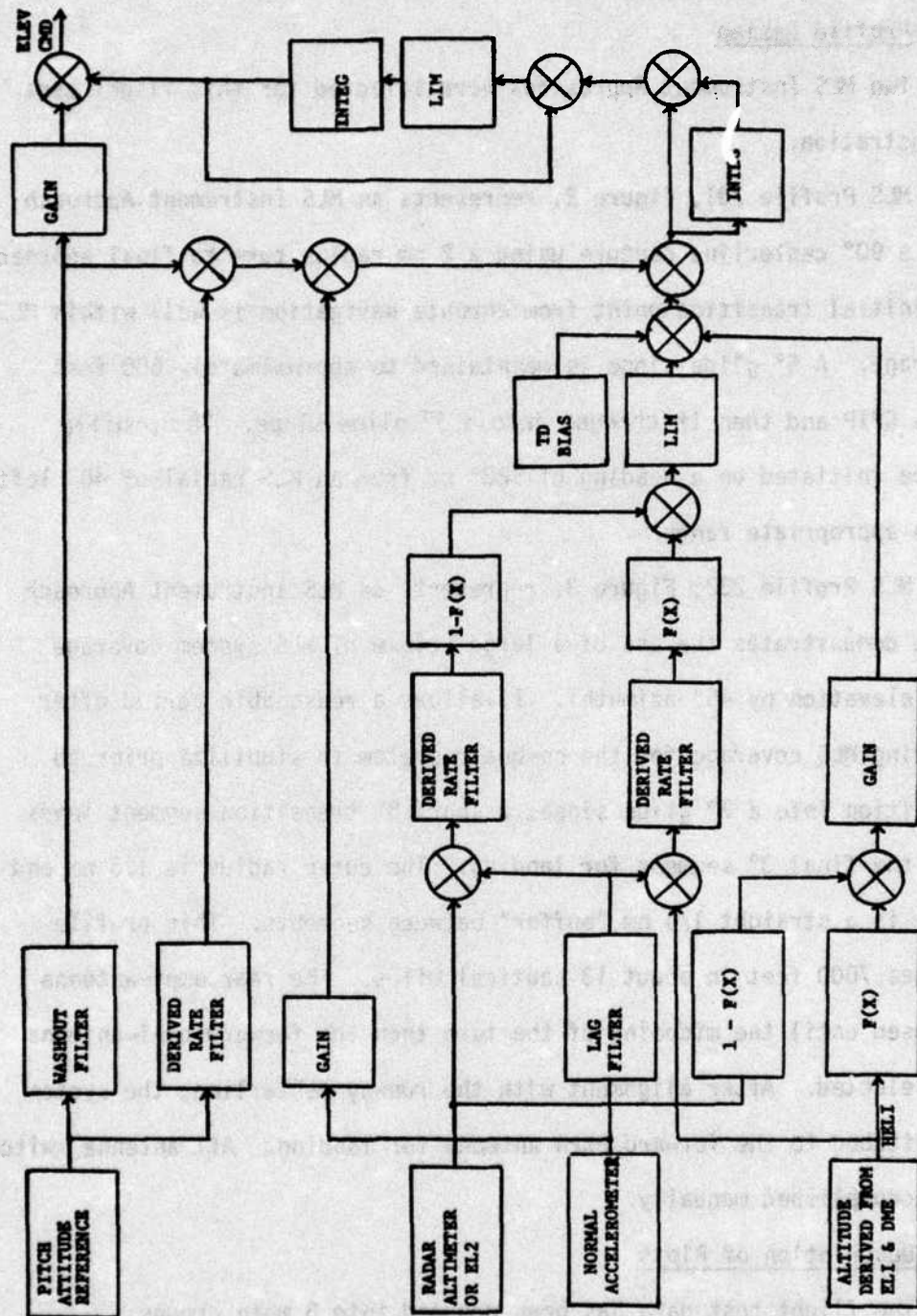


FIGURE 1 - T-39 MLS FLARE CONTROL LAW

force the aircraft to adhere to the intended program.

1.4 Profile Design

Two MLS Instrument Approaches were selected for this flight test demonstration.

MLS Profile 231, Figure 2, represents an MLS Instrument Approach with a 90° centerline capture using a 2 nm radius turn to final approach. The initial transition point from enroute navigation is well within MLS coverage. A 5° glide slope is maintained to approximately 600 feet above GPIP and then it changes into a 3° glide slope. The profile can be initiated on a heading of 128° or from an MLS radial of 40° left at an appropriate range.

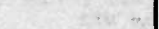
MLS Profile 232, Figure 3, represents an MLS Instrument Approach which demonstrates the use of a large volume of MLS system coverage (18° elevation by 45° azimuth). It allows a reasonable period after entering MLS coverage for the on-board system to stabilize prior to transition into a 7° glide slope; a short 5° transition segment leads into the final 3° segment for landing. The curve radius is 1.5 nm and there is a straight 1/4 nm "buffer" between segments. This profile changes 7000 feet in about 13 nautical miles. The rear omni-antenna was used until the midpoint of the turn then the forward omni-antenna was selected. After alignment with the runway centerline, the system is switched to the forward horn antenna for landing. All antenna switching was accomplished manually.

1.5 Description of Plots

The flight test data has been grouped into 3 main groups:

(1) Landing Accuracy Data - This group provides information relative to aircraft system performance based on phototheodolite data.

City, New Jersey:



MLS PROFILE NO. 232

NAFEC ATLANTIC CITY
ATLANTIC CITY, NEW JERSEY

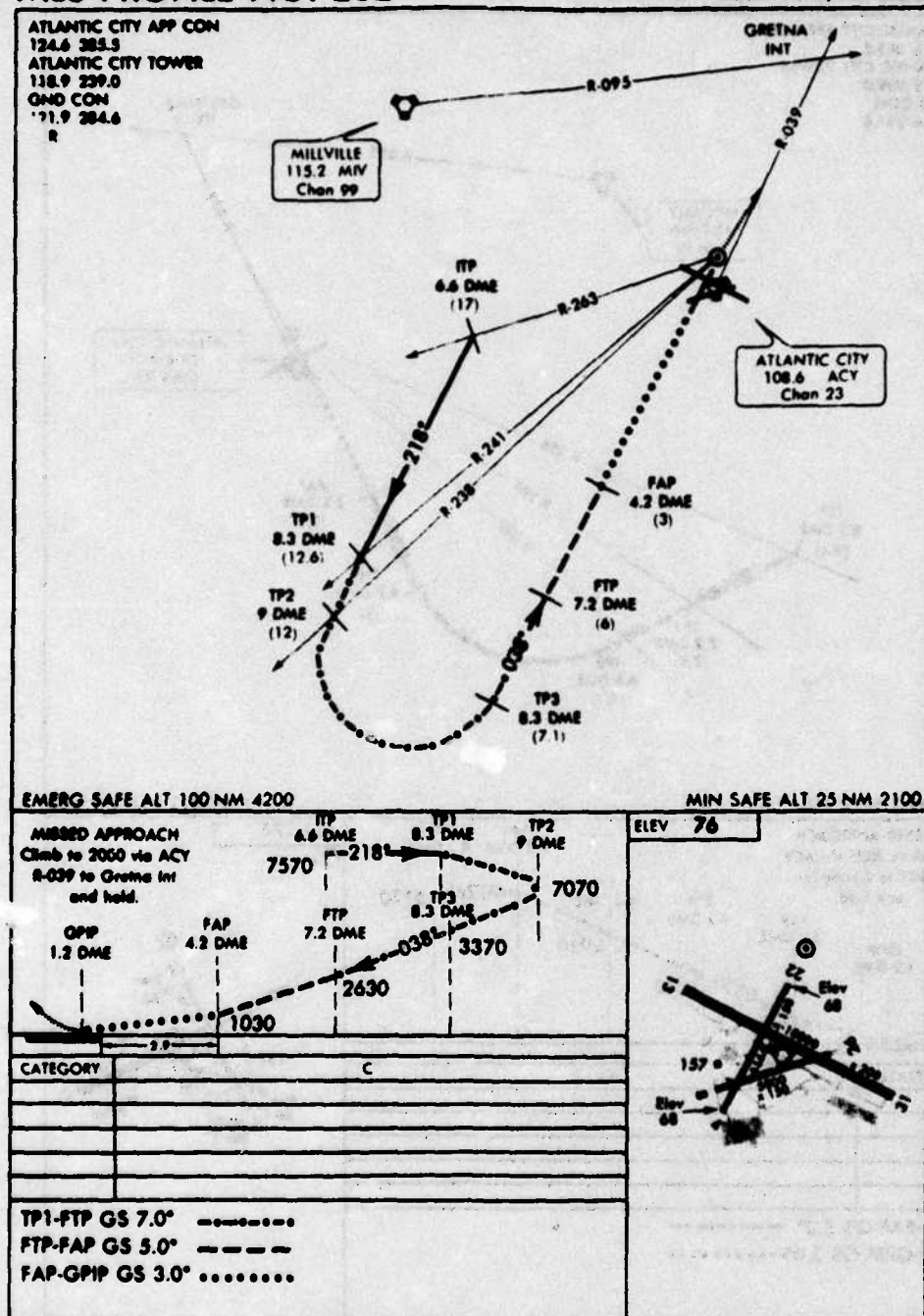


FIGURE 3 - MLS PROFILE 232

(2) MLS Accuracy Data - This group provides information on MLS accuracy in the final approach and landing zone.

(3) Profile Accuracy Data - This group provides information relative to total system performance in flying curved and segmented MLS Instrument Approaches.

1.5.1 Landing Accuracy Data

Phototheodolite data¹ has been plotted to evaluate aircraft system performance during automatic MLS landings. The plots represent vertical path, horizontal path, vertical velocity and touchdown dispersions. The abscissa of the first 3 plots, ground range from threshold, has been divided into 32 partitions of 304 feet and the mean ordinate value within each partition has been plotted. Significant points of the approach to landing have been marked on the horizontal path plot representing 100 Foot Decision Height, Threshold, Glide Path Intercept Point (GPIP) and Touchdown. A solid line has been drawn on the vertical path plot to represent a 3° glide slope.

The touchdown dispersion plot summarizes the performance of the aircraft landing system for each of the flare techniques. The touchdown point is plotted as the lateral position from the runway centerline against an expanded scale of range from threshold.

1.5.2 MLS Accuracy Data

Graphs have been plotted for each automatic landing to establish the accuracy of the MLS data: azimuth angle error, elevation angle error,

¹ The Phototheodolite data used in this program was processed with a round earth tilt algorithm as opposed to the more accurate spheroid tilt algorithm; consequently height errors of up to 1.8 feet in threshold region are possible.

range error and height error. Phototheodolite data¹ was used to establish the true position of the aircraft and compared with the MLS data recorded on board the aircraft at a sample rate of 5 times per second. Azimuth angle, elevation angle and range are direct outputs from the MLS receiver while aircraft height is calculated on board the aircraft from MLS received data. The abscissa of the graphs, ground range from threshold, has been divided into 32 partitions of 304 feet to form a bucket of information; the mean error and 2σ points during each bucket have been plotted at the center of the partition. The bars at the end of each mean value define the $\pm 2\sigma$ values for each bucket. If no data is received during a bucket, then no plot is made.

As data from the ELI transmitter becomes unreliable at small elevation angles, the elevation angle error and height error plots have been terminated once the aircraft reaches 50 ft altitude. The DME calibration was checked and set to zero on the DME receiver indicator before each flight to ensure that both the phototheodolite and DME were referenced to the nose of the aircraft. A calibration error value of -97.9 feet was applied to all DME data. This error was the difference between DME received and phototheodolite at the runway calibration point. It should be noted that this calibration also eliminated the normal system tolerances.

1.5.3 Profile Accuracy Data

Summary profile plots are presented which superimpose all data runs of a particular profile on single horizontal (X-Y) and vertical (Z-ATK) plot. The along track distance (ATK) is defined as the remaining distance to go along the desired track. On the data plots, although X

and Y coordinates are plotted together to show horizontal tracks, X versus Z is no longer adequate for vertical track. Z versus ATK shows the true glide slope along the curved path. The X axis represents the extended runway centerline and remains positive. The Y axis is left or right of the runway centerline as seen by the pilot on final approach. Right is positive and left is negative. The Z axis is the vertical distance from the GPIP as measured along the datum flight path. The datum flight path (desired path) is indicated by the continuous line. The circles identify the various transition points shown in Figure 2 and 3. As aircraft track is based on received MLS data (indicated by the dotted line), tracking errors represent total system performance including MLS errors.

SECTION 2.0 FLIGHT TEST RESULTS

2.1 Elevation Antenna (EL1) Fade-In to Radio Altimeter Flare

The data presented in this section represents a typical approach using MLS Profile 232 and automatic landing using EL1 Fade-in to radio altimeter flare.

2.1.1 Vertical Tracking

Figure 4 is a typical phototheodolite vertical tracking plot. The aircraft was tracking slightly high of glide slope at 1 nm from threshold and on glide slope at 1/2 nm from threshold to the flare point of 43 feet above GPIIP. The tendency to fly high on the glide slope could be accounted for by the height error generated by the DME calibration error described in section 1.0. Vertical height (calculated from EL1 and DME) is used for the entire profile vertical path until flare is initiated on radio altimeter.

2.1.2 Lateral Tracking

A typical phototheodolite lateral tracking plot is shown in Figure 5. The MLS azimuth accuracy was a factor in accomplishing good lateral tracking in the approach and landing zone. Key points of the approach are identified as 100 foot Decision Height, Threshold, GPIIP and Touchdown.

2.1.3 Vertical Velocity

A typical plot of the T-39 vertical velocity, based on phototheodolite data, is presented in Figure 6. The aircraft is flying a 3° glide slope requiring approximately 12 fps rate of descent at the airspeed being flown. Touchdown is programmed to occur at approximately 2.5 fps rate of descent; a touch and go landing was accomplished.

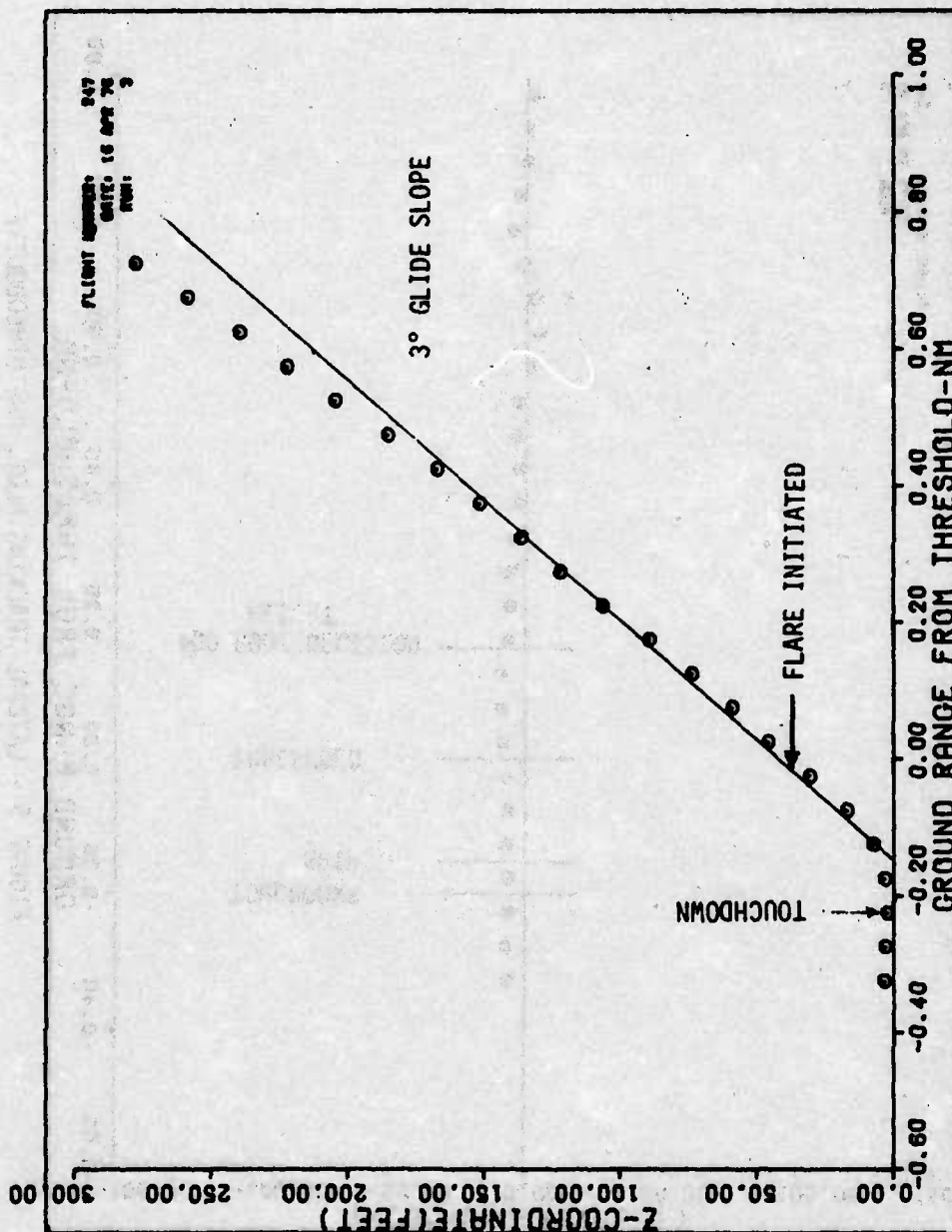


FIGURE 4 - VERTICAL TRACKING PLOT, PHOTOTHEODOLITE
(RADIO ALTIMETER FLARE)

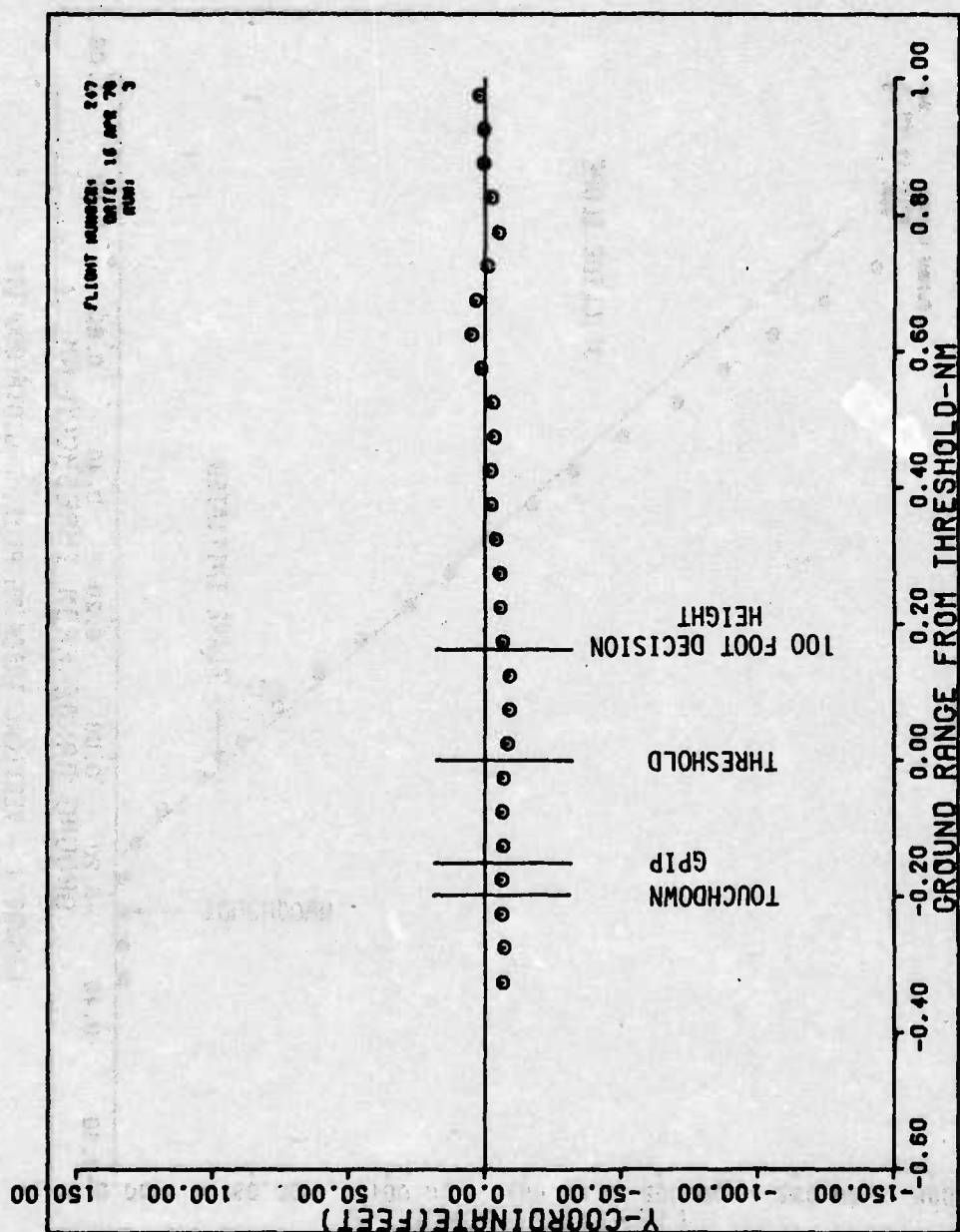


FIGURE 5 - LATERAL TRACKING PLOT, PHOTO THEODOLITE
(RADIO ALTIMETER FLARE)

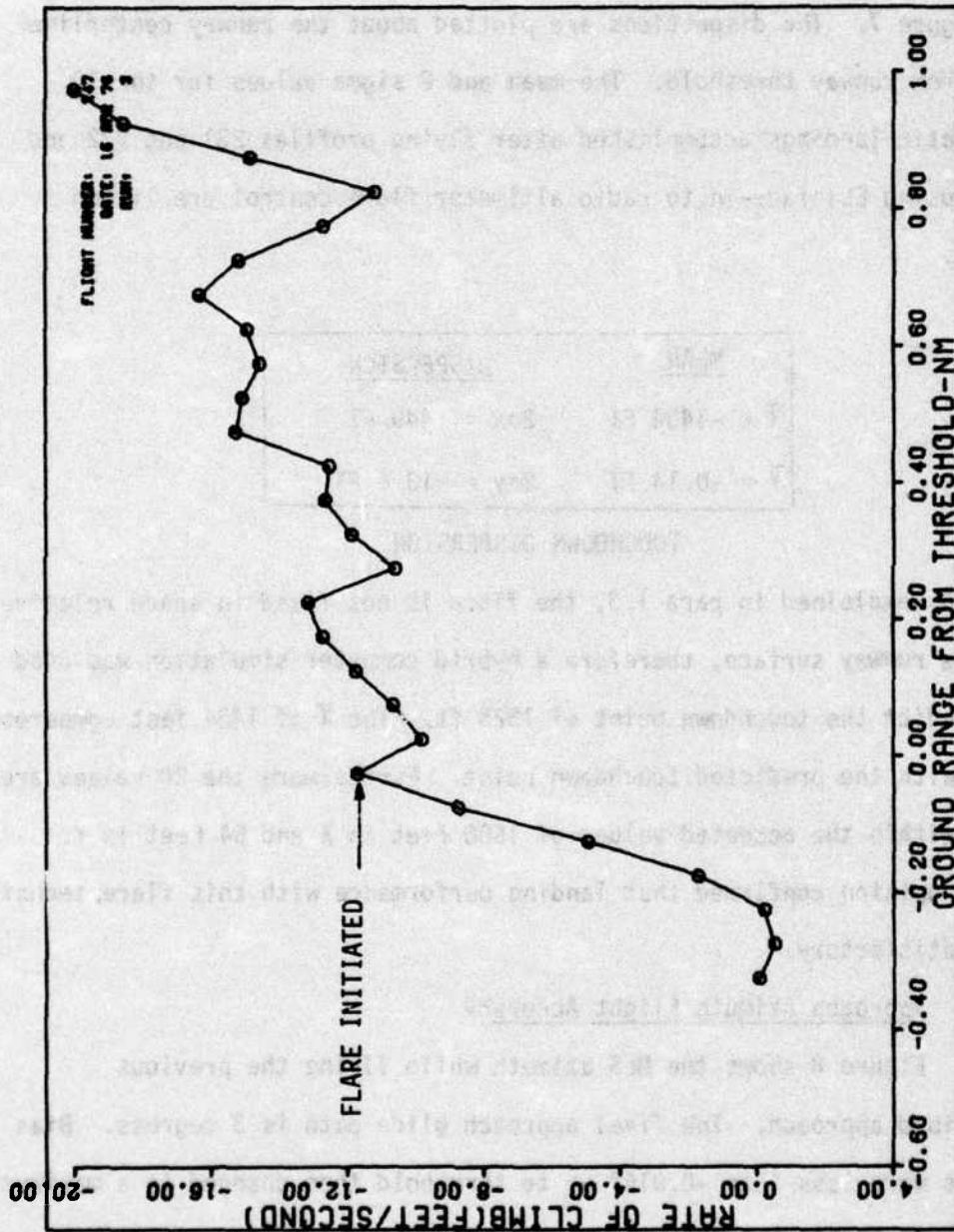


FIGURE 6 - T-39 VERTICAL VELOCITY, PHOTOTHEODOLITE
(RADIO ALTIMETER FLARE)

2.1.4 Automatic Touchdown Landing Dispersion

The lateral and longitudinal runway touchdown points are presented in Figure 7. The dispersions are plotted about the runway centerline and from runway threshold. The mean and 2 sigma values for the 10 automatic landings accomplished after flying profiles 231 and 232 and then using EL1 fade-in to radio altimeter flare control are listed below.

<u>MEAN</u>	<u>DISPERSION</u>
$\bar{X} = -1434 \text{ FT}$	$2\sigma_x = +449 \text{ FT}$
$\bar{Y} = -0.14 \text{ FT}$	$2\sigma_y = +13.6 \text{ FT}$

TOUCHDOWN DISPERSION

As explained in para 1.3, the flare is not fixed in space relative to the runway surface, therefore a hybrid computer simulation was used to predict the touchdown point of 1525 ft. The \bar{X} of 1434 feet compares well with the predicted touchdown point. Furthermore the 2σ values are well within the accepted values of 1500 feet in X and 54 feet in Y. Pilot opinion confirmed that landing performance with this flare technique was satisfactory.

2.1.5 Approach Azimuth Flight Accuracy

Figure 8 shows the MLS azimuth while flying the previous described approach. The final approach glide path is 3 degrees. Bias errors were less than -0.015° up to threshold then changed to a maximum value of $+0.03^\circ$ at $-.13 \text{ nm}$ from threshold. The noise error $\pm 2\sigma$ value was 0.04° peak variation near threshold.

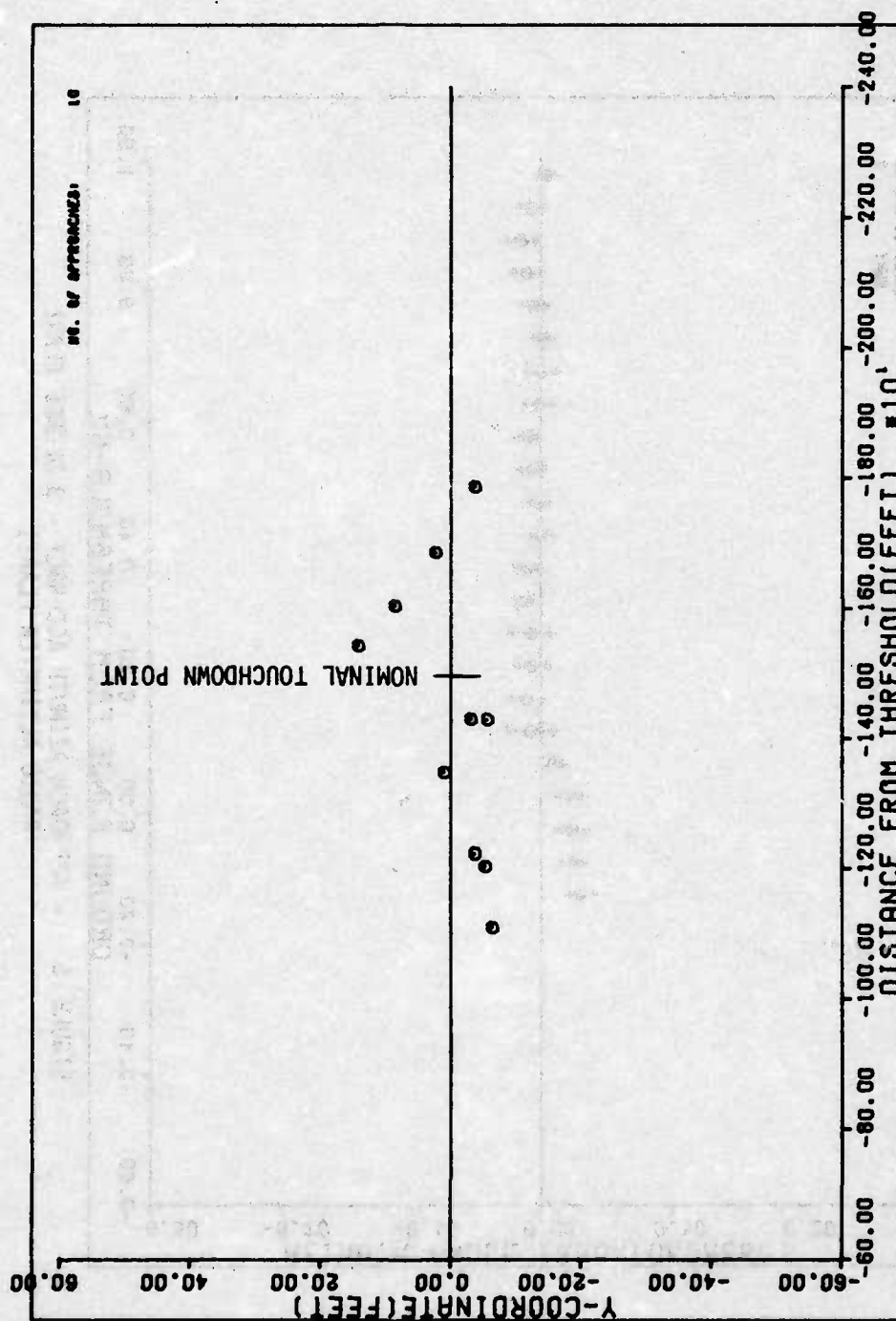


FIGURE 7 - AUTOMATIC LANDING TOUCHDOWN DISPERSION
(RADIO ALTIMETER FLARE)

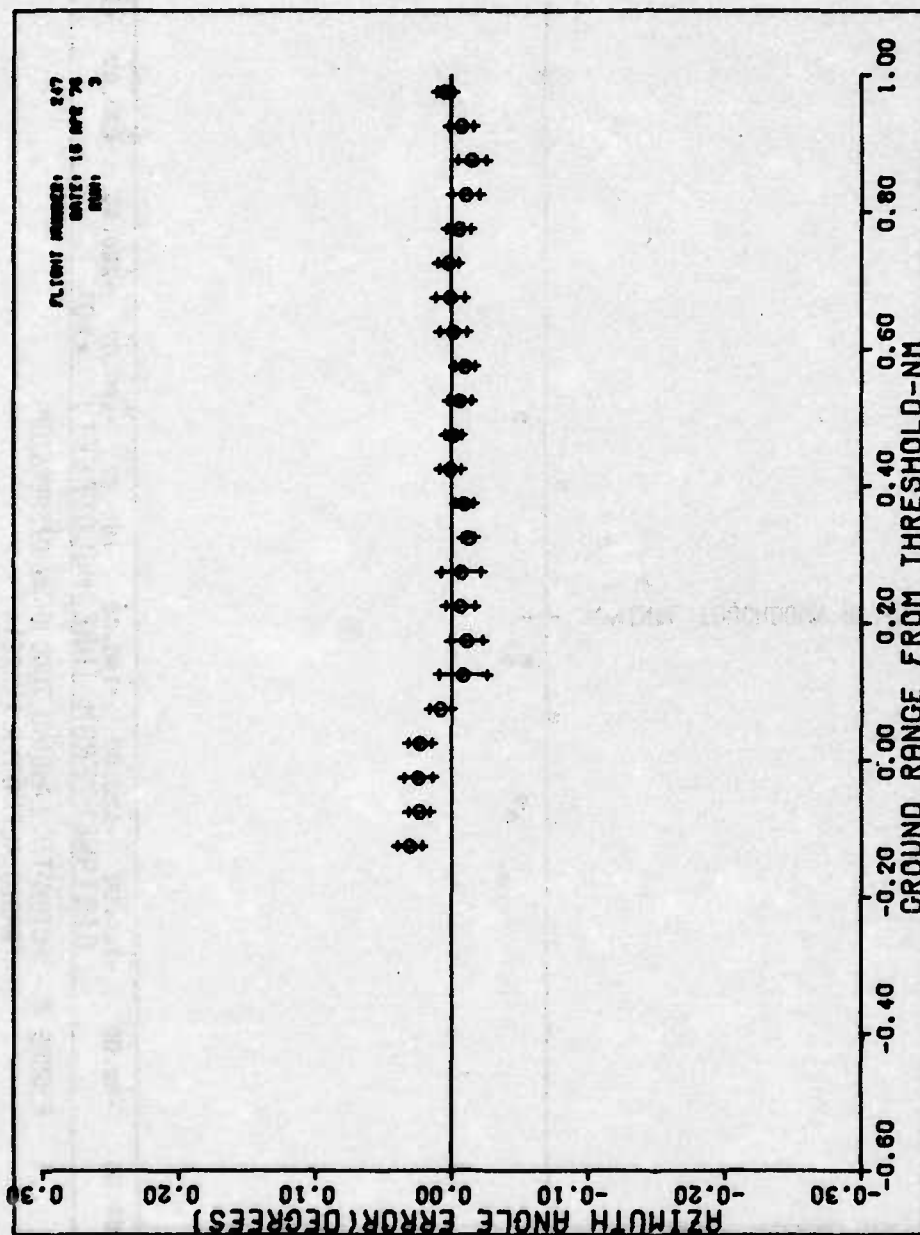


FIGURE 8 - APPROACH AZIMUTH ACCURACY - 3 DEGREE FLARE
(RADIO ALTIMETER FLARE)

2.1.6 Elevation Flight Accuracy

The elevation 1 accuracy is shown in Figure 9. The elevation bias from 1.0 to 0.3 nautical miles varied from -0.005° to -0.03° and increased to -0.15° at threshold. The $\pm 2\sigma$ noise error was normally 0.03° from 1.0 to 0.3 nautical miles; however the $\pm 2\sigma$ noise error started to increase at the 100 foot elevation point reaching 0.15° at threshold (50 foot elevation).

2.1.7 Range Flight Accuracy

Figure 10 shows the range accuracy. The bias was normally +3 meters except around the threshold region where it changed to -2 meters. The $\pm 2\sigma$ noise error was normally 8 meters but increased to 17 meters at threshold.

2.1.8 Height

Figure 11 is a typical height error plot. The height error is the MLS height (derived from EL1 and DME) minus the phototheodolite tracking height. The height error characteristics are similar to those of the MLS EL1 and DME error.

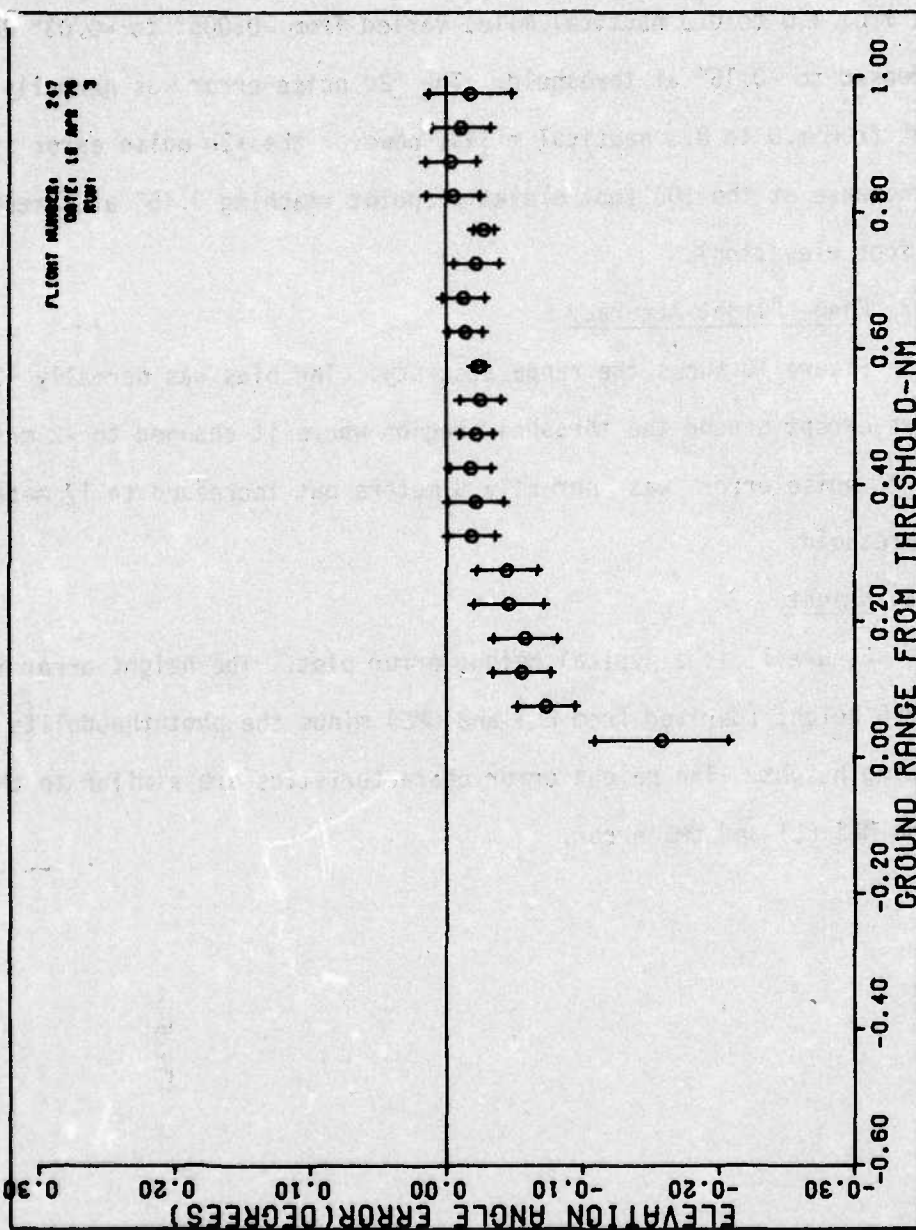


FIGURE 9 - ELEVATION 1 ACCURACY - 3 DEGREE APPROACH
(RADIO ALTIMETER FLARE)

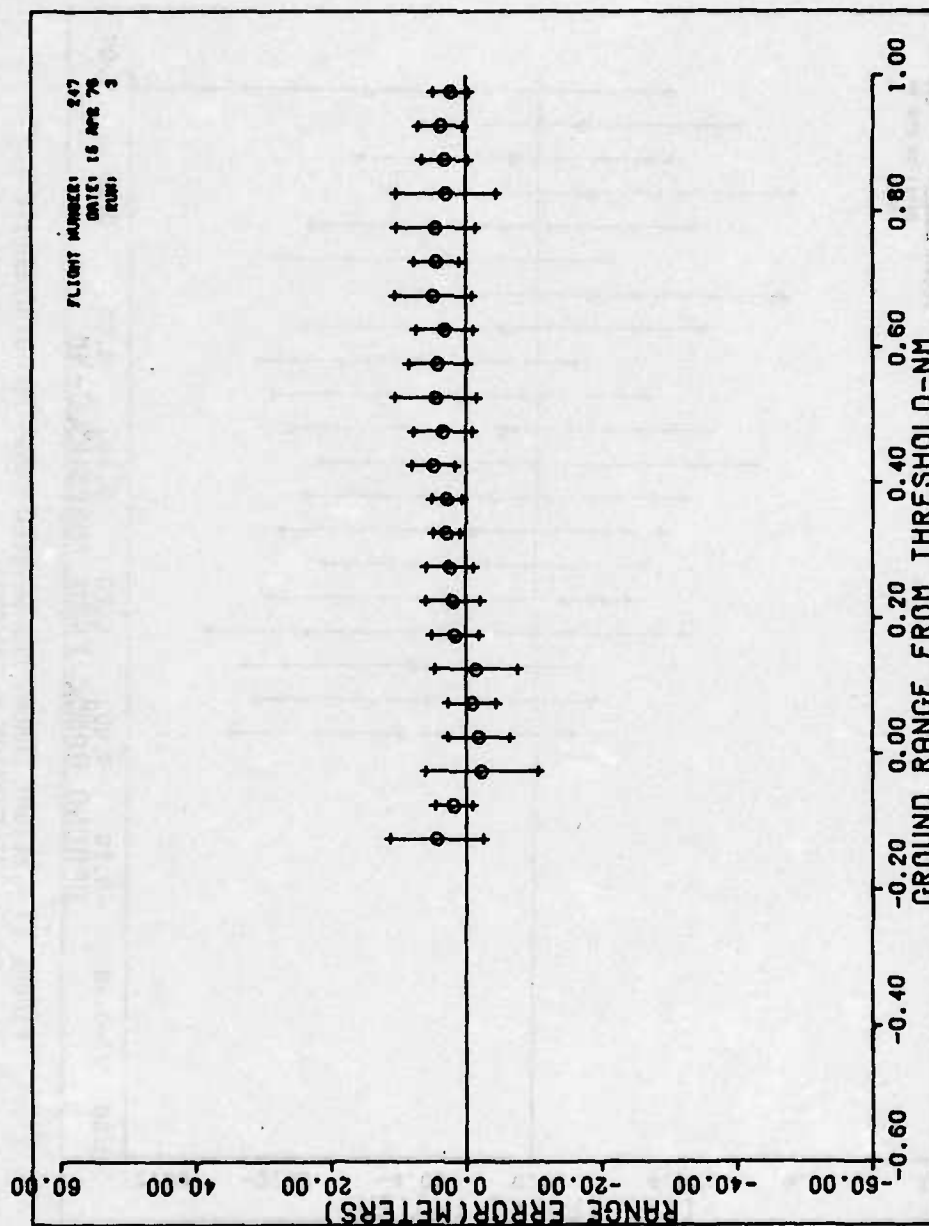


FIGURE 10 - RANGE ACCURACY - 3 DEGREE APPROACH
(RADIO ALTIMETER FLARE)

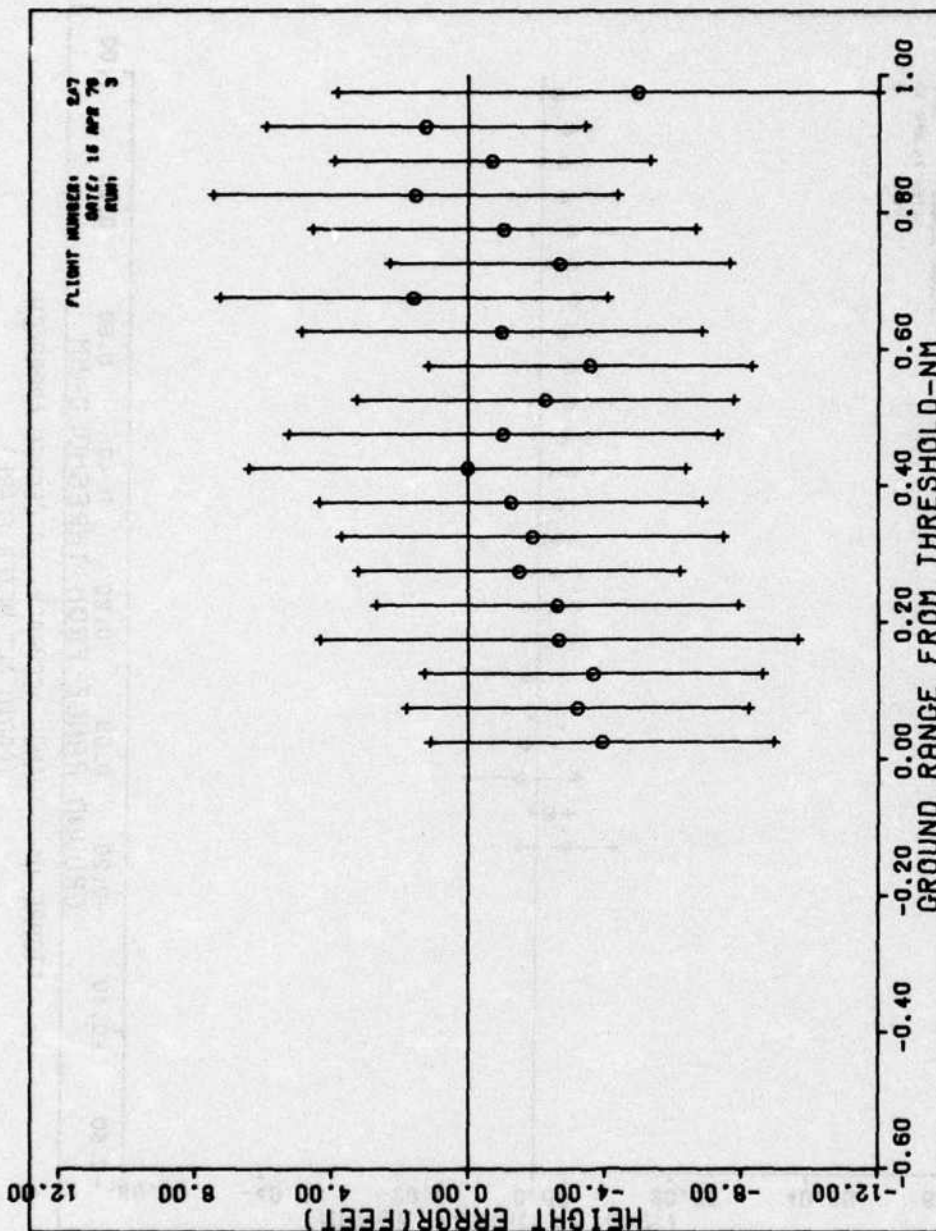


FIGURE 11 - HEIGHT ERROR, MLS DERIVED MINUS PHOTO THEODOLITE
(ELEVATION 1 AND DME)

2.2 Flare Antenna (EL2) Flare

The data presented in this section represents a typical approach which was obtained on April 22, Run 2 using MLS Profile 232 and automatic landing using EL2 flare.

2.2.1 Vertical Tracking Plot

Figure 12 shows a typical EL2 flare vertical tracking plot based on phototheodolite data. The aircraft tends to level off at approximately 0.1 nm down the runway then lands slightly long. This tendency seems to correspond to the point where the EL2 error becomes larger and goes negative. The pilots reported that prior to touchdown the aircraft pitched slightly up, leveled off and then landed long.

2.2.2 Lateral Tracking Plot

A typical phototheodolite lateral tracking plot for an EL2 flare is shown in Figure 13, the 100 Foot Decision Height, Threshold, GPIP, and Touchdown are identified on the plot. Lateral tracking errors could have been affected by the surface winds which were from the left with an 8 knot tail wind component.

2.2.3 Vertical Velocity Plot

Figure 14 is a typical plot of T-39 vertical velocity during an EL2 flare approach; the plot is based on phototheodolite data. Flare is initiated over threshold at a rate of descent of approximately 12 fps. The rate of descent is decreased to approximately 2 fps at touchdown.

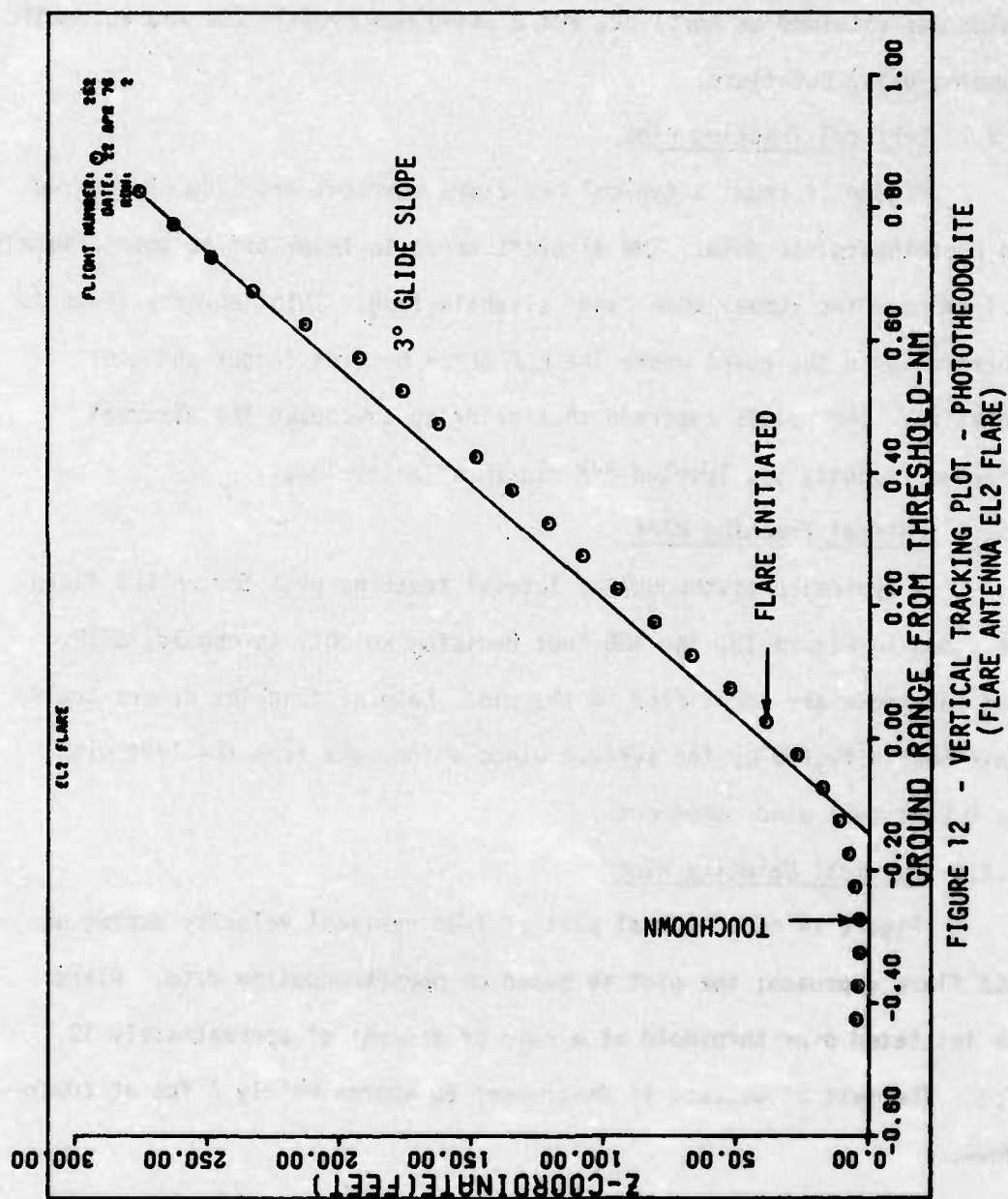


FIGURE 12 - VERTICAL TRACKING PLOT - PHOTOTHEODOLITE
(FLARE ANTENNA EL2 FLARE)

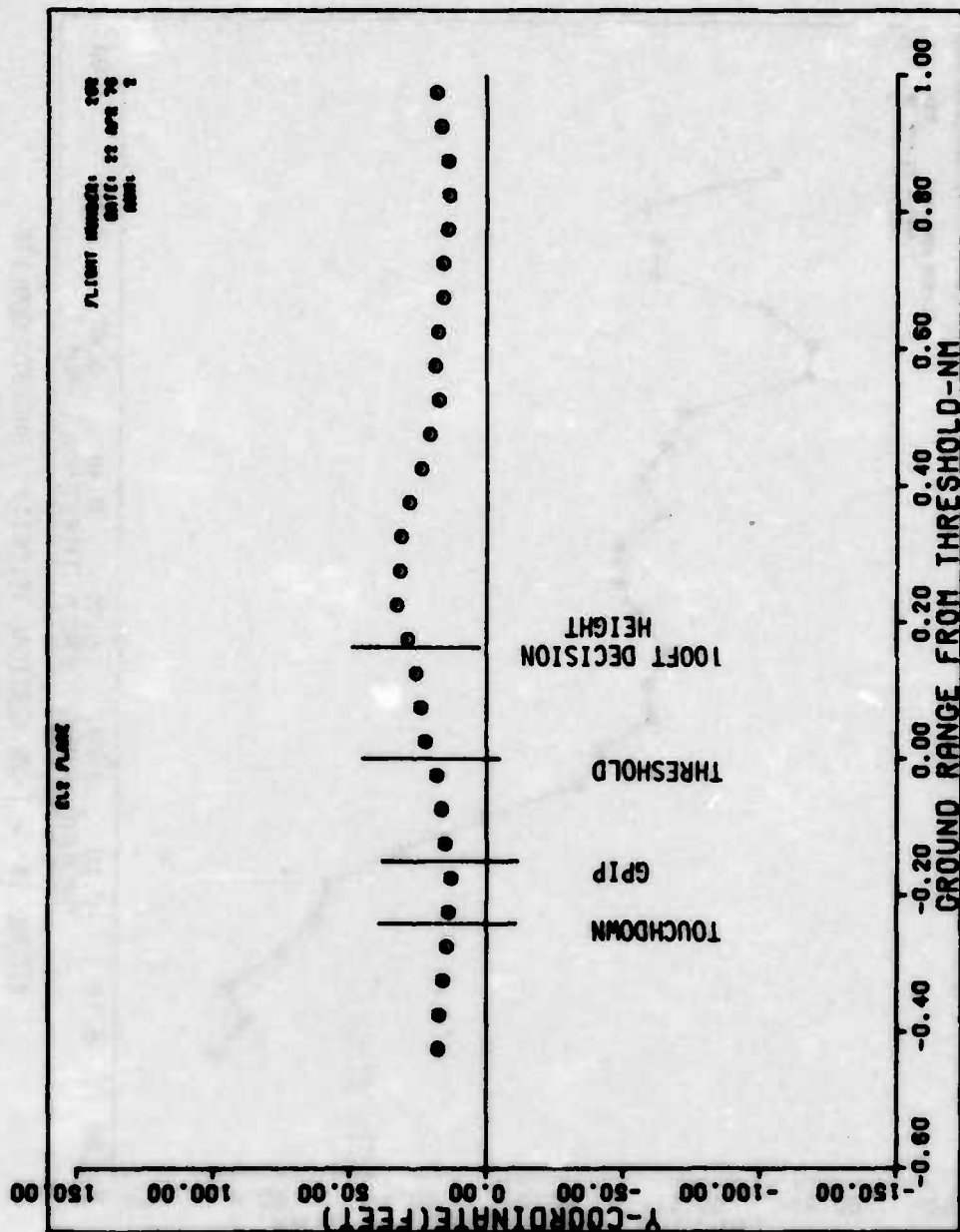


FIGURE 13 - LATERAL TRACKING PLOT - PHOTOTHEODOLITE
(FLARE ANTENNA EL2 FLARE)

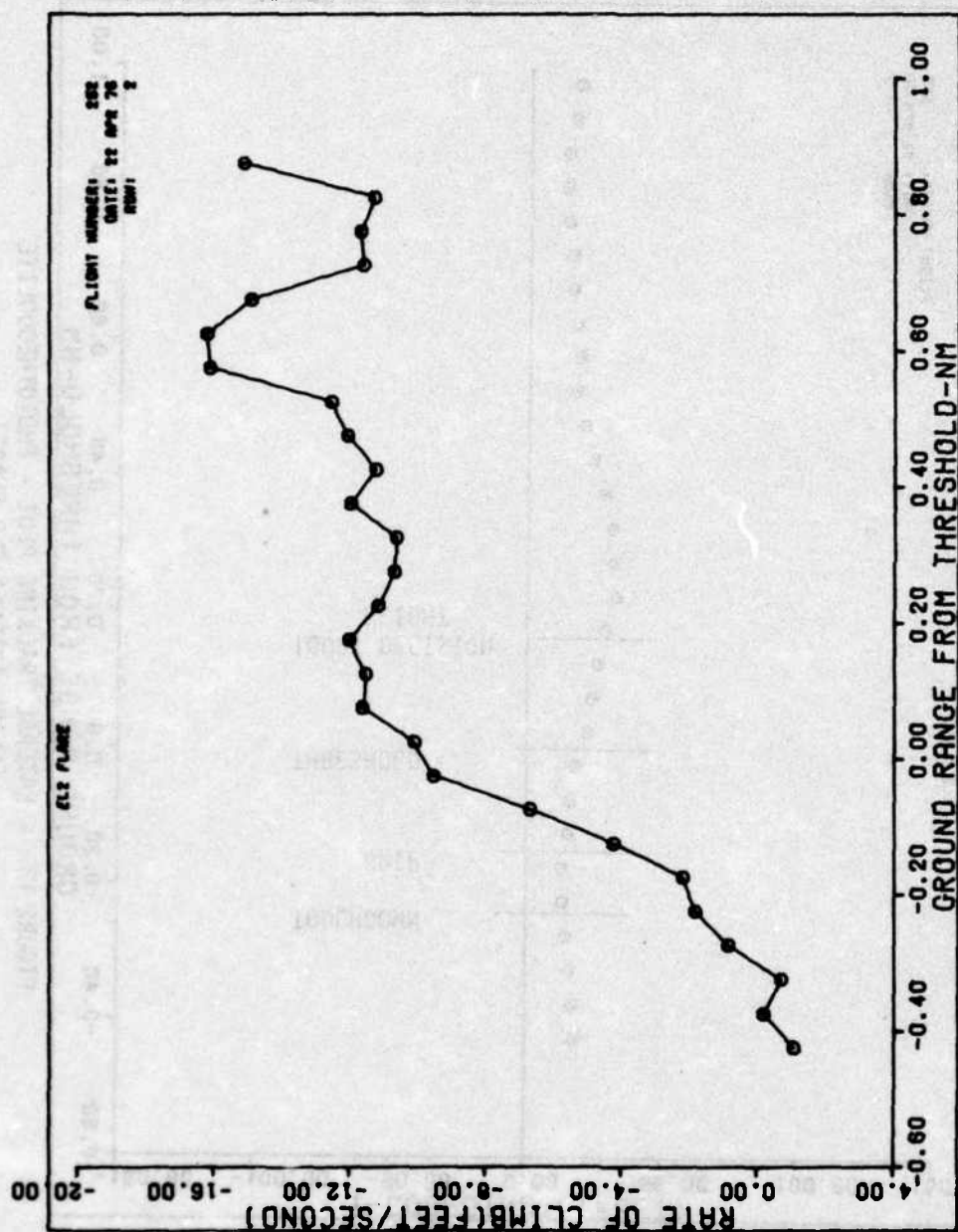


FIGURE 14 - T-39 VERTICAL VELOCITY - PHOTOTHEODOLITE
(FLARE ANTENNA EL2 FLARE)

2.2.4 Automatic Touchdown Landing Dispersion Plot

The presentation of landing touchdown points (Figure 15) are identical to that described for EL1 fade-in to radio altimeter. The mean and 2-sigma values for the 10 automatic landings performed after flying profiles 231 and 232 and using EL1 fade-in to EL2 flare technique are listed below.

<u>MEAN</u>	<u>DISPERSION</u>
$\bar{X} = -1843 \text{ FT}$	$2\sigma_x = +820 \text{ FT}$
$\bar{Y} = -0.86 \text{ FT}$	$2\sigma_y = +13.34 \text{ FT}$
<u>TOUCHDOWN DISPERSION</u>	

Although the 2-sigma value of lateral dispersion is within the accepted standard of 54 feet, the longitudinal dispersion using this technique is worse than that obtained using the EL1 fade-in to radio altimeter flare control. The mean touchdown point is 300 feet displaced from the nominal touchdown point and the dispersion is greater than the 1500 feet required. The plots of vertical path (Figure 12) indicate that the aircraft is leveling off and flaring high. Pilot opinion indicated that as the aircraft approaches touchdown the aircraft pitched slightly up and attempted to level off above the runway; the resulting landings using EL2 flare techniques were considered marginal by the pilots. Although inspection of the EL2 error data (Figure 17) shows negative values of 0.06 and 0.08 degrees of bias error in the flare and landing region, this equates to an approximate height of 2.4 feet which alone would not account for the high flare. Initial analysis is not conclusive as to the cause

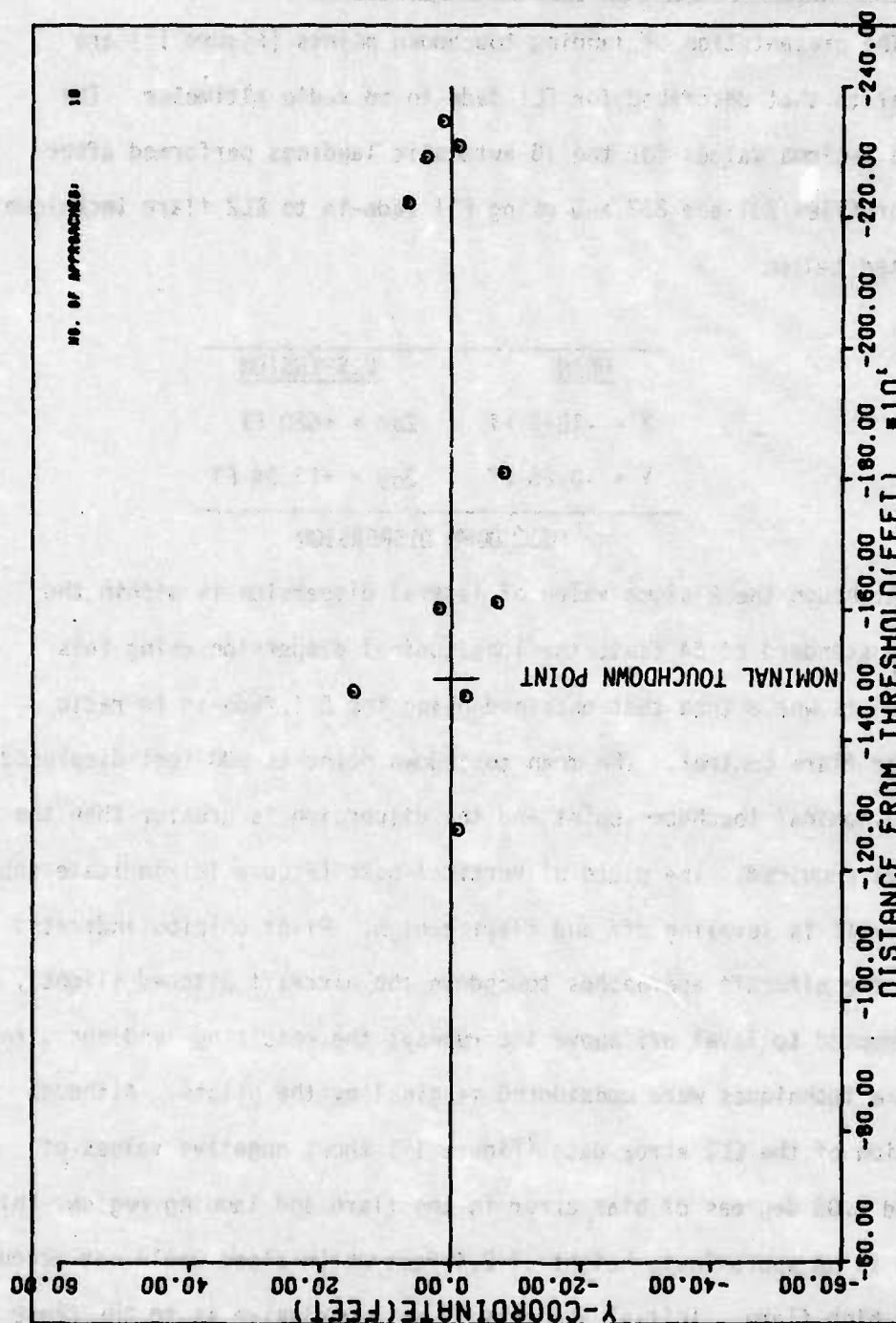


**FIGURE 15 - AUTOMATIC LANDING TOUCHDOWN DISPERSION
(ELEVATION 2 FLARE)**

of high flares on EL2 data, which are not experienced on radio altimeter flares. However the noise in both DME and EL2 is producing significant variance in derived height and as EL2 is not filtered in the T-39 aircraft system, this could be a contributing factor to the poor EL2 flare performance.

2.2.5 Approach Azimuth Flight Accuracy

Figure 16 shows the MLS azimuth accuracy while flying the previously described approach using EL2 flare technique. The accuracy data was similar to that described in section 2.1.5 for radio altimeter flare technique.

2.2.6 Flare Elevation 2 Flight Accuracy

The flare elevation 2 accuracy is shown in Figure 17. The elevation bias from 1.0 nautical miles to threshold varied from $+0.009^\circ$ to -0.04° . However, bias increased rapidly from threshold to the landing zone to -0.095° . The $\pm 2\sigma$ noise ranged from 0.08° to 0.19° up to the landing zone.

2.2.7 Range Flight Accuracy

Figure 18 shows the range accuracy obtained on the selected approach. The accuracy data characteristics were similar to those described in section 2.1.7 for radio altimeter flare technique.

2.2.8 DME Transients

Detailed analysis of DME data in the landing zone showed that range transients of up to 190,000 feet occurred lasting 0.2 seconds, see table 1; no MLS invalid flags were received during these transients. As DME is used in conjunction with MLS data to calculate aircraft position

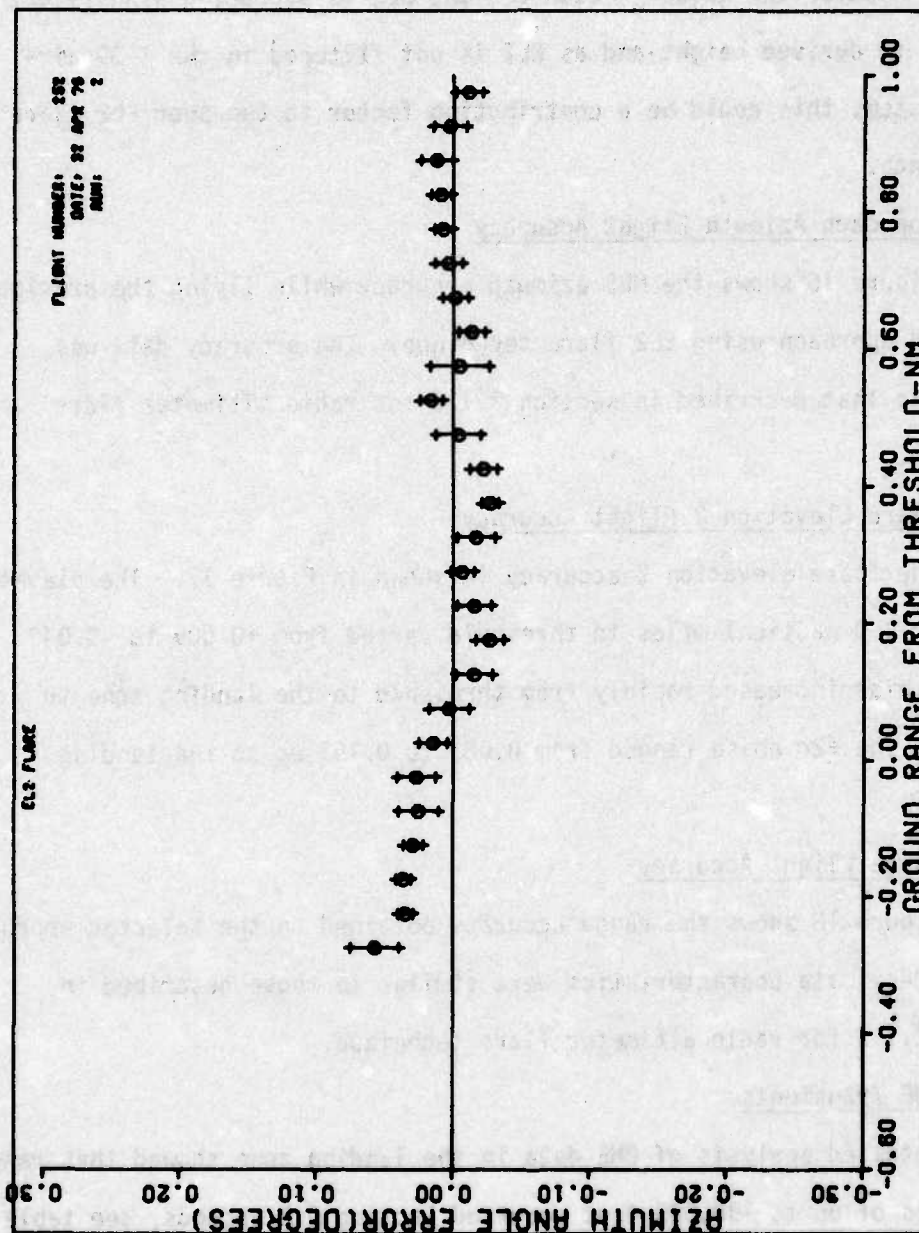


FIGURE 16 - APPROACH AZIMUTH ACCURACY - 3 DEGREE APPROACH

(FLARE ANTENNA EL2 FLARE)

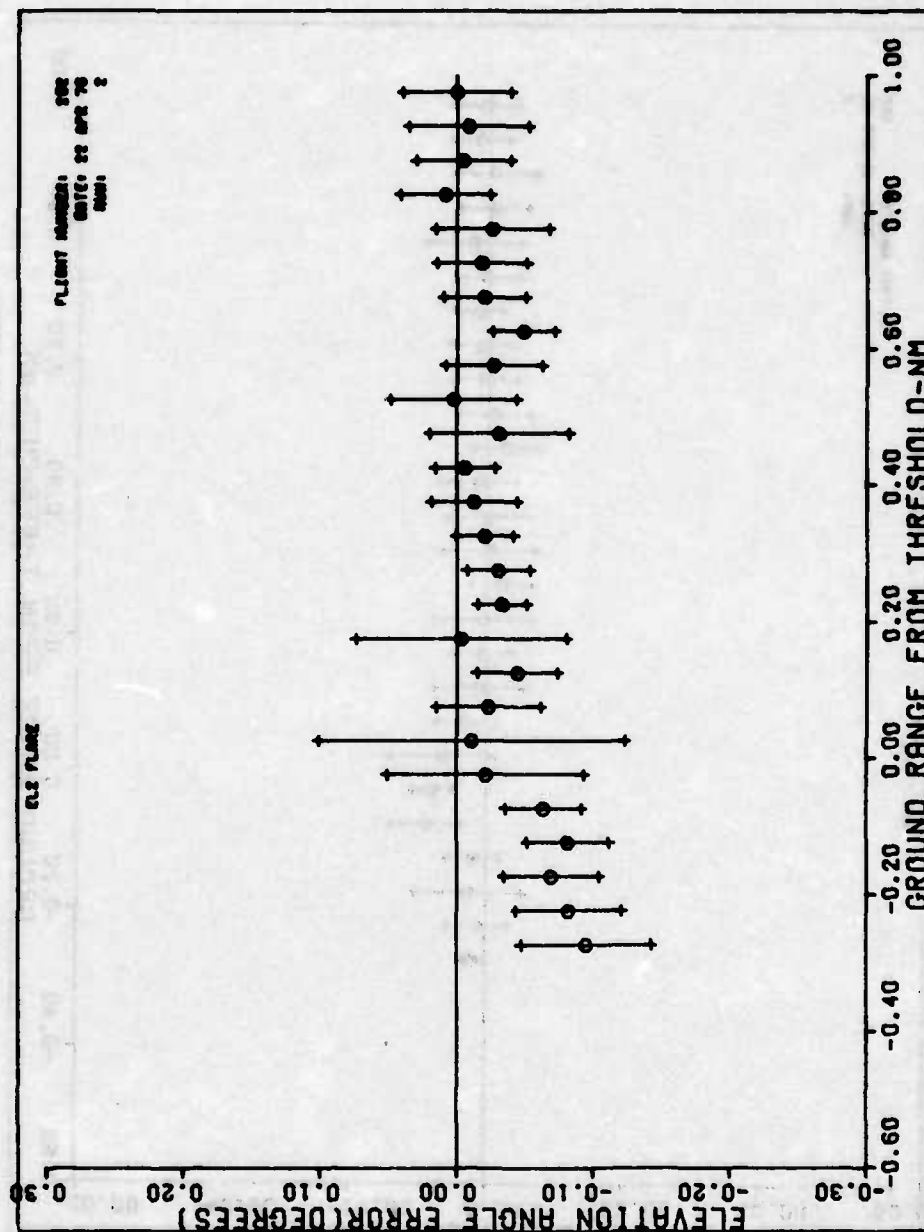


FIGURE 17 - ELEVATION 2 ACCURACY - 3 DEGREE APPROACH
(FLARE ANTENNA EL2 FLARE)

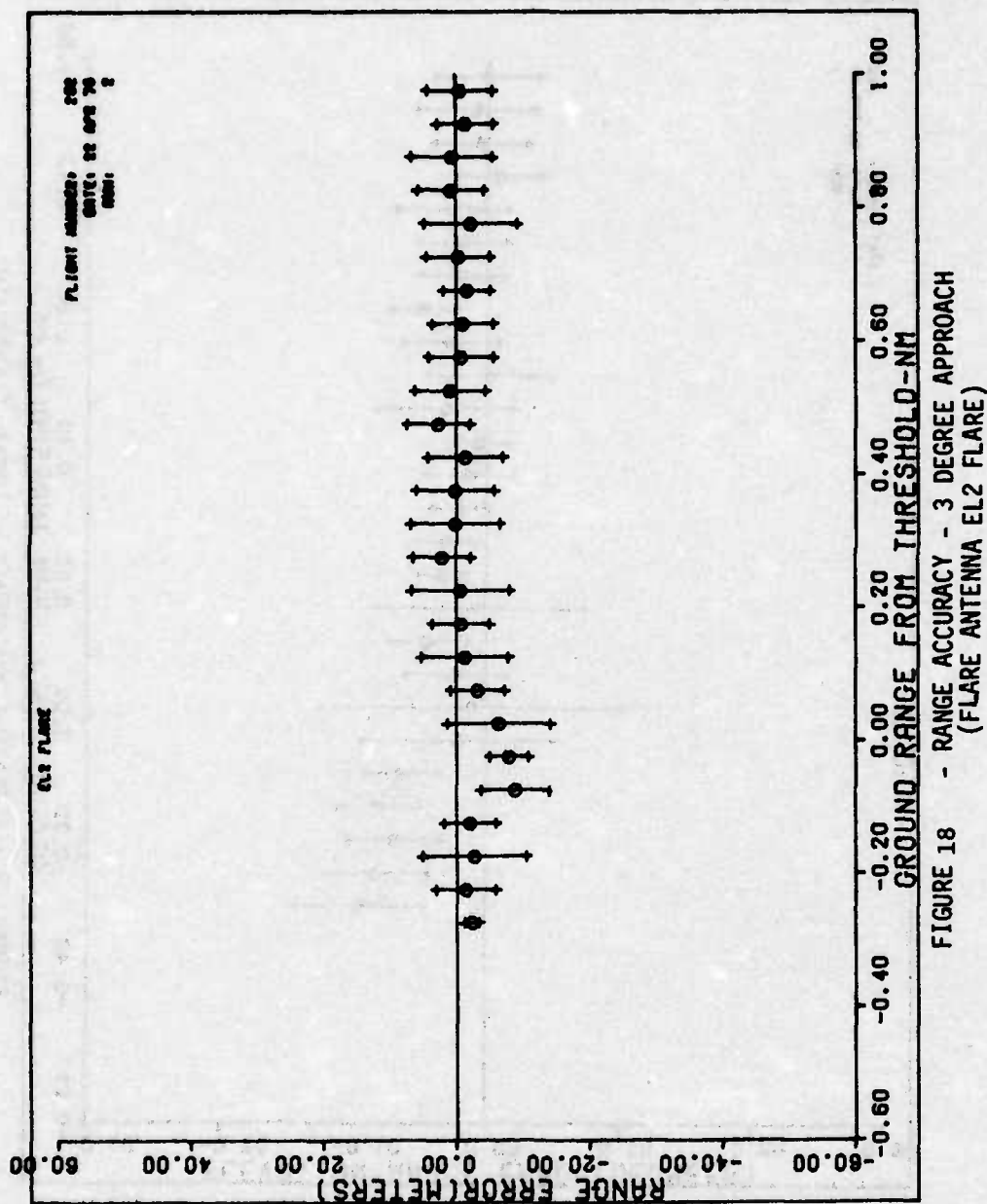


Table 1
RANGE TRANSIENTS AT GPIP

TIME	MLS AZIMUTH	DEG	MLS EL2	DEG	MLS RANGE	FT
10:53:00.480	.714133E-01		.433973E+00		.772905E+04	
10:53:00.580	.714133E-01		.373546E+00		.768651E+04	
10:53:00.680	.714133E-01		.373546E+00		.768651E+04	
10:53:00.780	.714133E-01		.307626E+00		.199102E+06*	
10:53:00.880	.714133E-01		.307626E+00		.199102E+06*	
10:53:00.980	.714133E-01		.280160E+00		.758929E+04	
10:53:01.080	.714133E-01		.280160E+00		.758929E+04	
10:53:01.180	.714133E-01		.280160E+00		.758929E+04	
10:53:01.280	.714133E-01		.280160E+00		.758929E+04	
10:53:01.380	.604266E-01		.252693E+00		.751030E+04	
10:53:01.480	.549333E-01		.274667E+00		.747992E+04	
10:53:01.580	.549333E-01		.175787E+00		.741916E+04	
10:53:01.680	.549333E-01		.175787E+00		.741916E+04	
10:53:01.780	.549333E-01		.192267E+00		.739485E+04	
10:53:01.880	.549333E-01		.192267E+00		.739485E+04	
10:53:01.980	.604266E-01		.137333E+00		.734017E+04	
10:53:02.080	.604266E-01		.137333E+00		.734017E+04	
10:53:02.180	.549333E-01		.824000E-01		.730978E+04	
10:53:02.280	.549333E-01		.824000E-01		.730978E+04	
10:53:02.380	.494400E-01		.933866E-01		.724902E+04	
10:53:02.480	.659200E-01		.549333E-01		.712142E+04	
10:53:02.580	.659200E-01		.549333E-01		.712142E+04	
10:53:02.680	.659200E-01		.384533E-01		.707281E+04	
10:53:02.780	.659200E-01		.384533E-01		.707281E+04	
10:53:02.880	.714133E-01		.494400E-01		.703635E+04	
10:53:02.980	.714133E-01		.494400E-01		.703635E+04	
10:53:03.080	.604266E-01		0.		.699989E+04	
10:53:03.180	.604266E-01		0.		.699989E+04	
10:53:03.280	.494400E-01		-.109867E-01		.696344E+04	
10:53:03.380	.494400E-01		-.109867E-01		.696344E+04	

Flight Number: 250

Date: 21 April 1976

Run: 7

*Typical Range Transient

relative to the runway, such transients can cause large errors in x, y, z typically 190,000 feet, 250 feet and 1000 feet. Since the height and crosstrack errors are direct inputs to the AFCS, auto pilot activity in this region due to DME transients can become hazardous. The effect of DME transients could be eliminated by introducing a DME reasonableness test to the digital program which would result in large DME transients being rejected.

2.3 Summary Plots of MLS Flight Accuracy

Summary plots of MLS data accuracy were made for the data approaches flown over a two week period. Twenty approaches are summarized for Azimuth, Range, and Elevation 1; ten approaches are summarized for Elevation 2 when EL2 flare technique was used for automatic landing.

2.3.1 Approach Azimuth Flight Accuracy

Figure 19 shows the MLS azimuth accuracy while flying 20 approaches over a two week period, the final approach glide path is 3 degrees. Bias errors were less than -0.02° up to threshold then changed $+0.04^\circ$ from threshold to the EL2 transmitter site. The noise error was normally a $\pm 2\sigma$ value of 0.04° with a peak variation of 0.08° at threshold.

2.3.2 Range Flight Accuracy

Figure 20 shows the range accuracy results from 20 approaches flown over a two week period. The bias was +2 meters except at threshold where it changed to -4 meters for approximately 600 feet of X distance; the bias increased to -6.5 meters approximately 6000 feet from the transmitter. The noise error, $\pm 2\sigma$, varies from 16 to 20 meters except at threshold and 0.4 nm from threshold where the variation ($\pm 2\sigma$) was 34 meters.

2.3.3 Elevation 1 Flight Accuracy

The elevation 1 accuracy is shown in Figure 21 for 20 approaches flown over a two week period. The elevation bias was normally -0.02° . The $\pm 2\sigma$ noise error was 0.06° to 0.1° from 1.0 to 0.2 nautical miles; the $\pm 2\sigma$ noise error changed rapidly at the 100 foot elevation point to 0.26° at threshold (50 foot elevation).

2.3.4 Flare Elevation 2 Flight Accuracy

The flare elevation 2 accuracy is shown in Figure 22 for ten approaches flown over a three day period. The elevation bias from 1.0 nautical miles to touchdown varied from -0.02° to -0.1° . The $\pm 2\sigma$ noise ranged from 0.09° to 0.13° up to the landing zone.

2.4 MLS Instrument Approaches

2.4.1 Profile 231

This MLS Instrument Approach, Figure 2, was flown 10 times with a fully coupled automatic control and automatic throttle system; Figures 23 and 24 are summary plots of horizontal and vertical tracks respectively. Although the aircraft system has the capability to fly RNAV on VORTAC into the MLS coverage, for the purpose of MLS testing this function was omitted and the aircraft was manually positioned at the initial transition point; thereafter the aircraft was flown purely on MLS. The 10 approaches show very little dispersion after the aircraft captures the horizontal and vertical flight paths. MLS data was available by the start of the profile (left 40° and 2700 feet above GPIP). The forward C-Band omni-antenna was used throughout each approach until the aircraft was steady on centerline, then the crew manually switched to the horn antenna. The C-Band horn was used for radio altimeter flare and the Ku-Band horn was

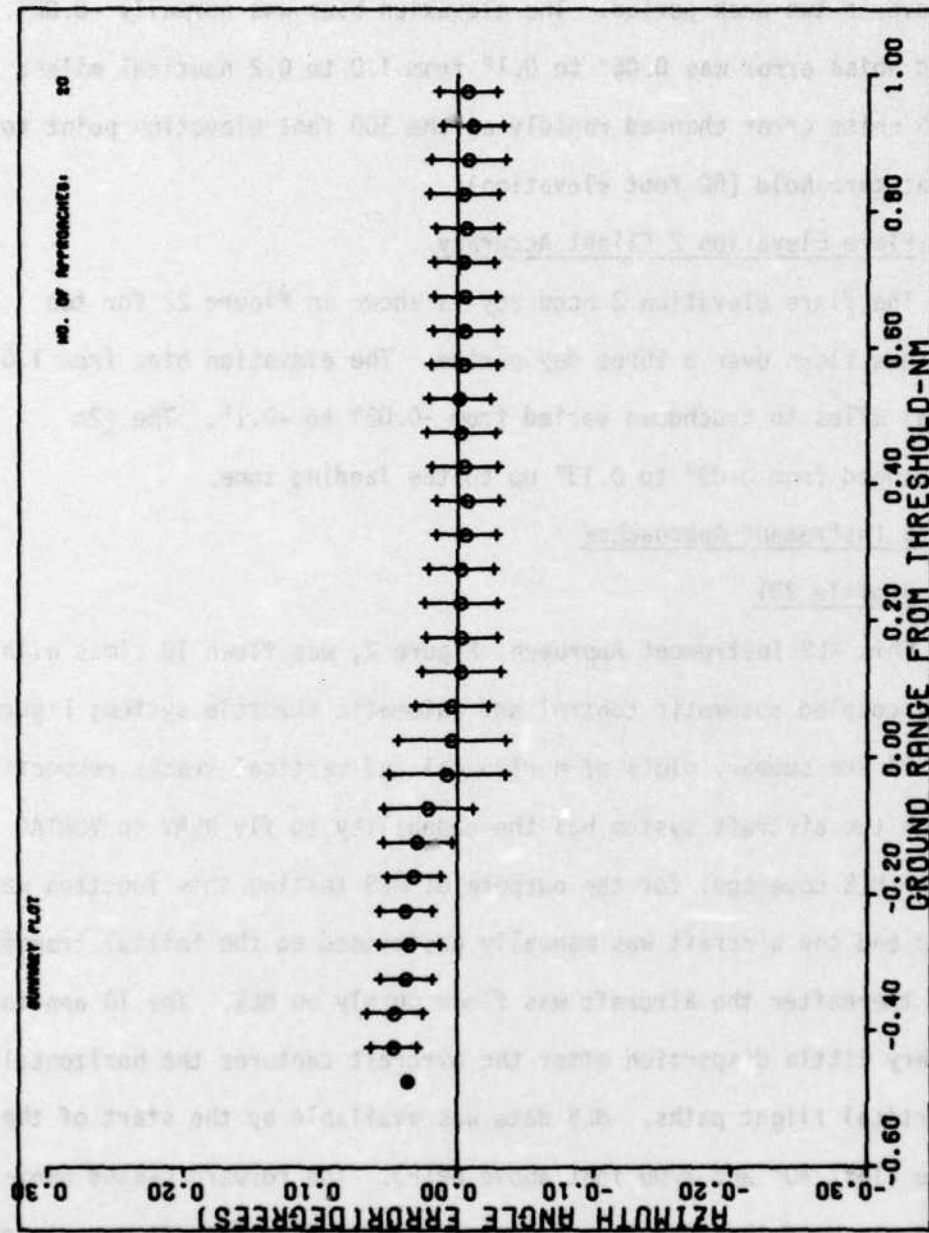


FIGURE 19 - APPROACH AZIMUTH ACCURACY, 3-DEGREE APPROACH
(SUMMARY PLOT, 20 APPROACHES)

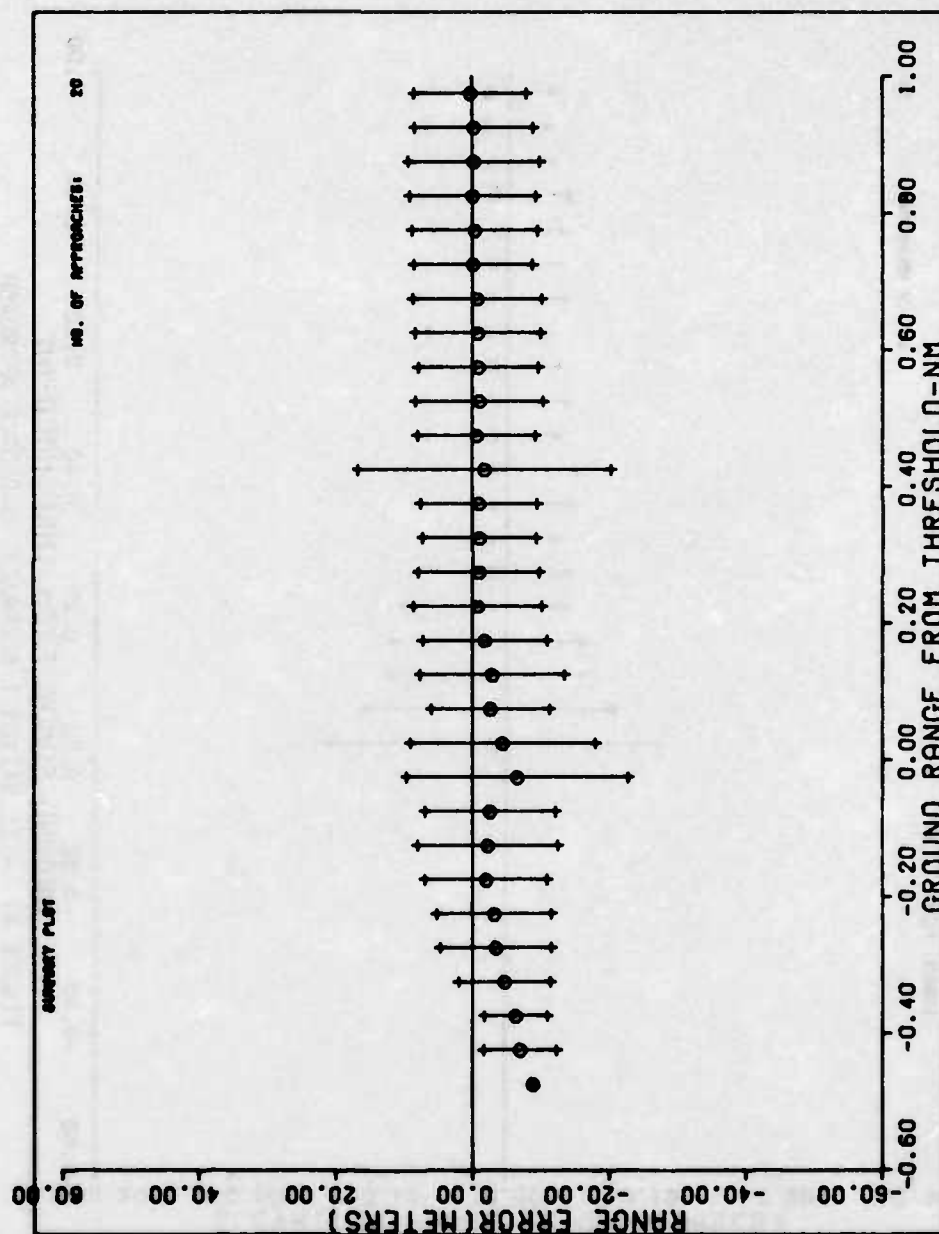


FIGURE 20 - RANGE ACCURACY, 3-DEGREE APPROACH
(SUMMARY PLOT, 20 APPROACHES)

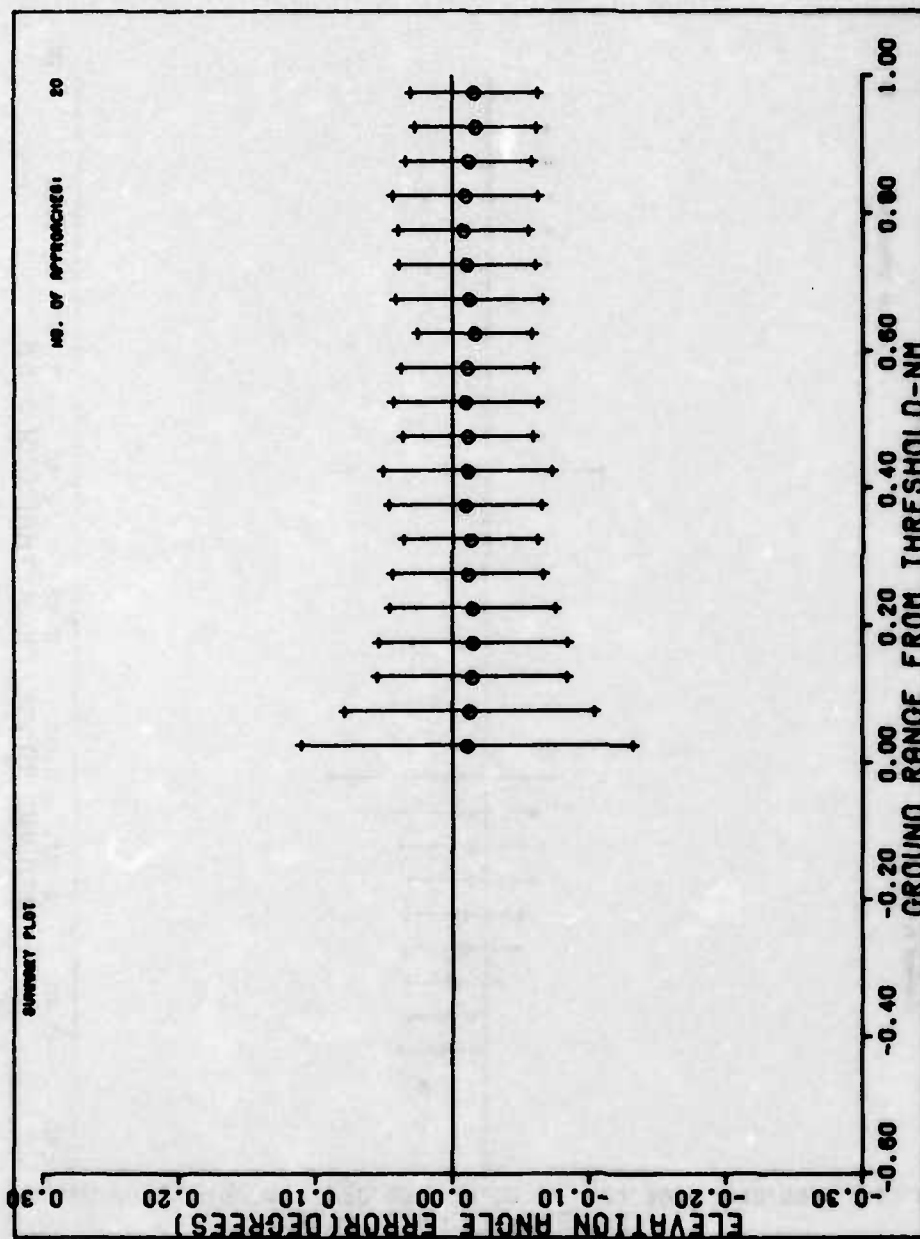


FIGURE 21 - ELEVATION 1 ACCURACY, 3-DEGREE APPROACH
(SUMMARY PLOT, 20 APPROACHES)

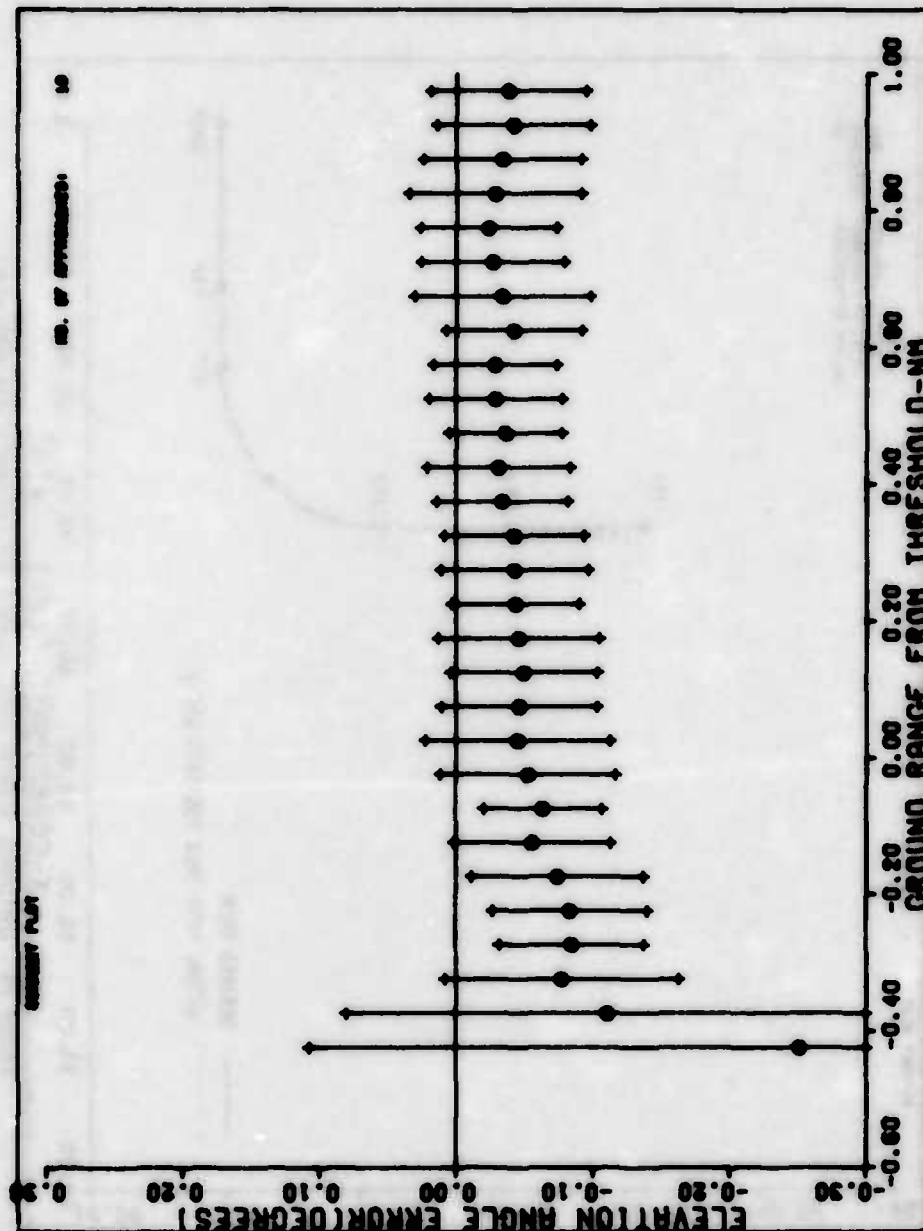


FIGURE 22 - ELEVATION 2 ACCURACY, 3-DEGREE APPROACH
(SUMMARY PLOT, 10 APPROACHES)

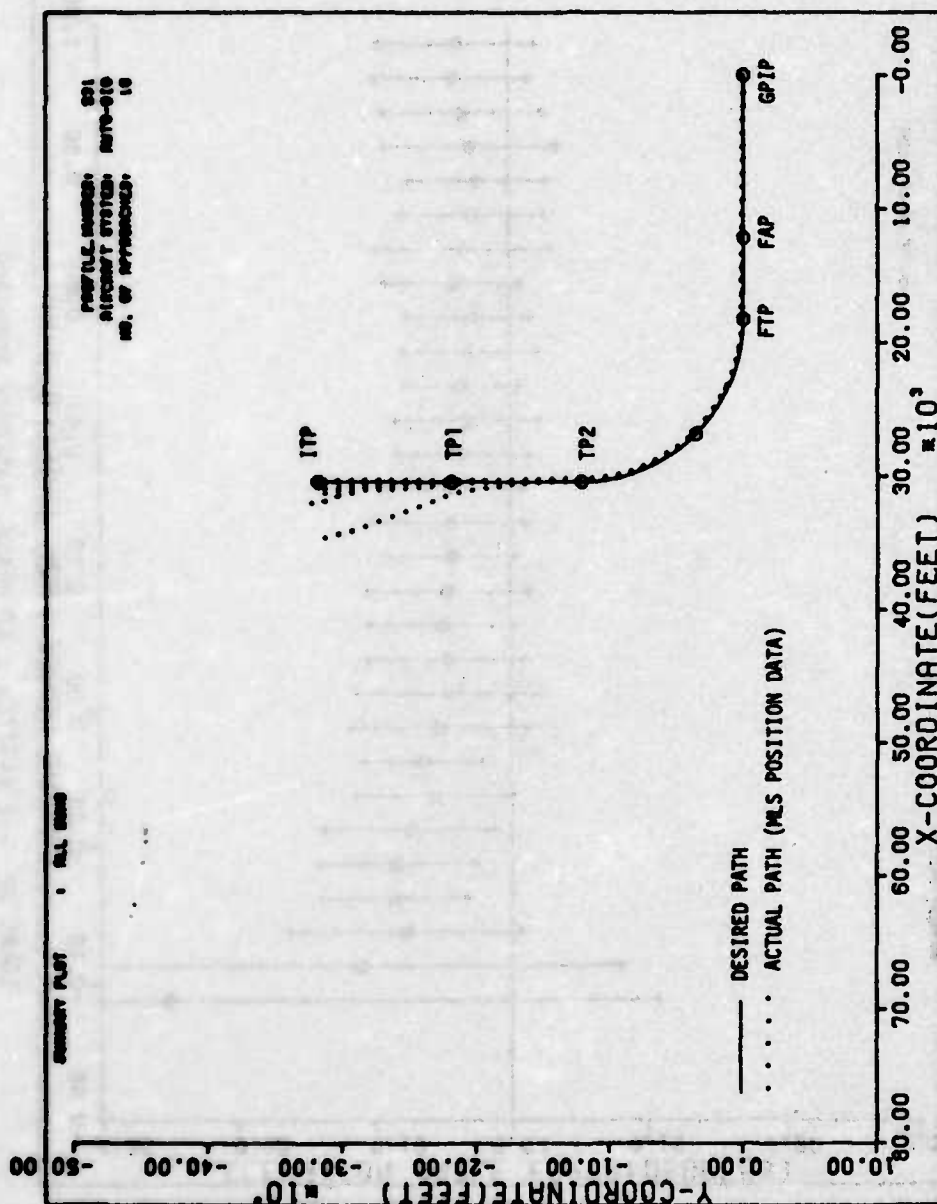


FIGURE 23 - HORIZONTAL SUMMARY PLOT, PROFILE 231, AUTOMATIC (10 APPROACHES)

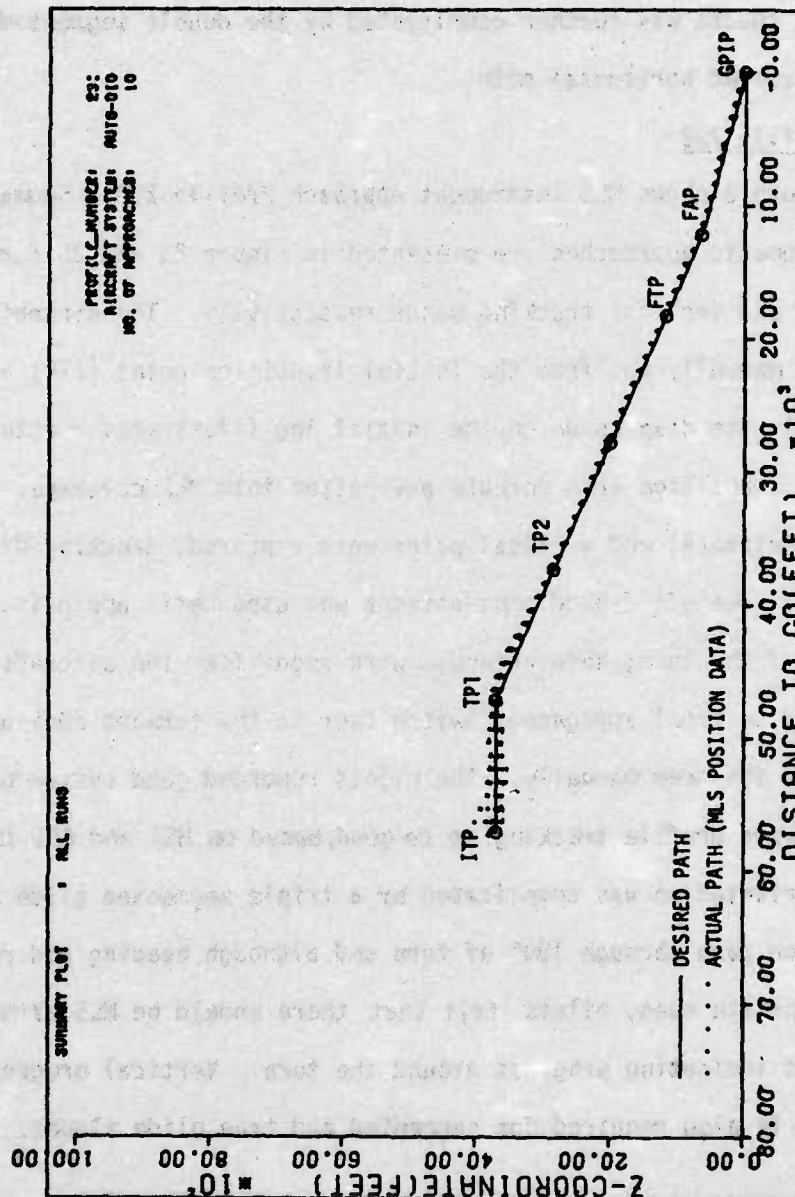


FIGURE 24 - VERTICAL SUMMARY PLOT, PROFILE 231, AUTOMATIC - (10 APPROACHES)

used for EL2 flare. Although the pilots felt confident in flying this approach and orientation was fairly good, they still felt that there should be an indication of MLS azimuth and elevation. Vertical orientation for height checks was further complicated by the double segmented glide slope and curved horizontal path.

2.4.2 Profile 232

Figure 3 shows MLS Instrument Approach Profile 232. Summary plots for 11 automatic approaches are presented in Figure 25 and 26 for the horizontal and vertical tracking paths respectively. The aircraft was positioned manually out from the initial transition point (ITP) as in Profile 231; the dispersion on the initial leg illustrates a potential problem of transition from enroute navigation into MLS coverage. However, once the horizontal and vertical paths were captured, tracking dispersions were small. The aft C-Band omni-antenna was used until approximately the mid-point of the turn; horn antennas were used after the aircraft was established on final approach. Switch over to the forward omni-antenna was made by the crew manually. The pilots reported good system performance and considered profile tracking to be good, based on HSI and ADI information. However, orientation was complicated by a triple segmented glide slope and a curved path through 180° of turn and although heading and range gave appropriate cues, pilots felt that there should be MLS azimuth angles cues indicating progress around the turn. Vertical progress monitoring is also required for segmented and true glide slopes.

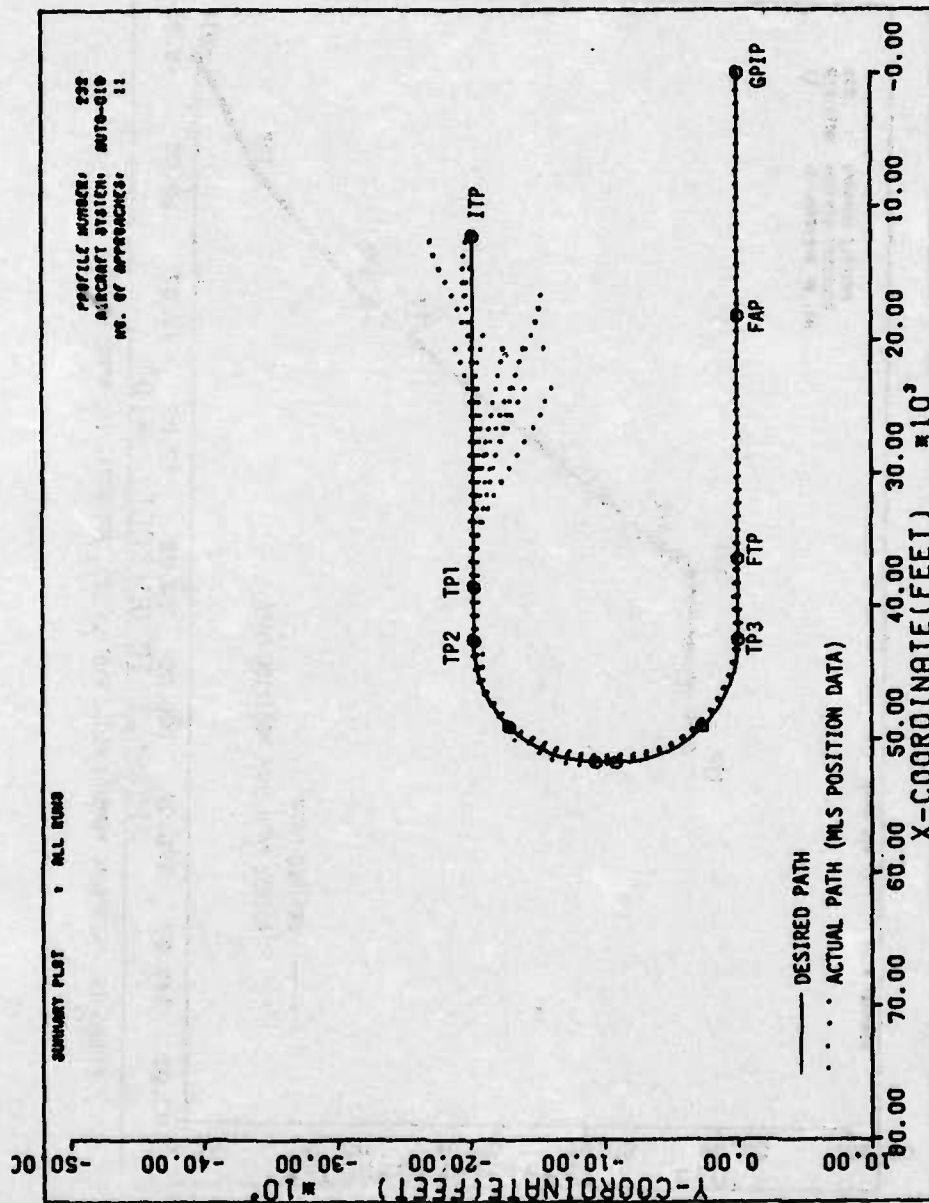


FIGURE 25 - HORIZONTAL SUMMARY PLOT, PROFILE 232, AUTOMATIC (10 APPROACHES)

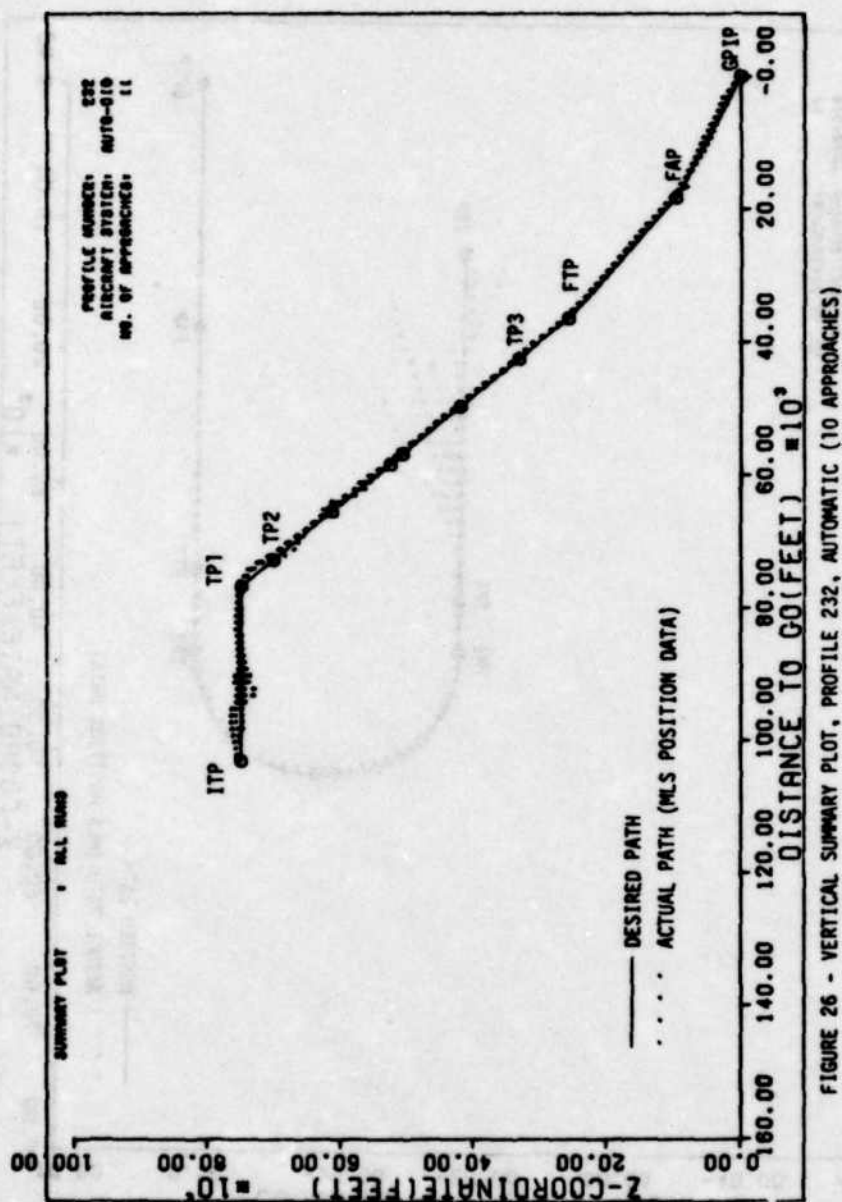


FIGURE 26 - VERTICAL SUMMARY PLOT, PROFILE 232, AUTOMATIC (10 APPROACHES)

SECTION 3.0 CONCLUSIONS

3.1 General

The purpose of this section is to present conclusions which have been discussed in detail elsewhere in this report. Following each statement is a reference to the section(s) of the report which provides explanation of technical points.

(1) Time Reference Scanning Beam Microwave Landing System provides adequate guidance to perform satisfactory automatic landings in the T-39 aircraft using Elevation Antenna (EL1) fade-in to radio altimeter flare technique. (Section 2.1)

(2) Flares are considered marginal using Elevation Antenna (EL1) fade-in to Flare Antenna (EL2) flare technique in the T-39 aircraft. This limitation was attributed to error in height calculations in the landing zone due to large range errors and EL2 variation as recorded in T-39 flight tests. (Section 2.2)

3.2 Judgment Conclusion

The above conclusions were based on limited data and analysis of flight test data. A more thorough flight test and analysis is required of aircraft performance integrated with MLS accuracy data. Aircraft performance and MLS accuracy data in the threshold (flare initiation region) and landing zone must be analyzed in depth to determine the effect of derived height variation resulting from MLS data.

APPENDIX A

DATA RETRIEVAL OF
ON-BOARD DATA AND PHOTOTHEODOLITE

I. MLS Data Scaling for On Board Recorder

1. MLS Azimuth, EL1 and EL2

full scale amplitude $\pm 180^\circ$

count slope 0.00549335°

2. Absolute Altitude from EL1

full scale amplitude ± 25000 feet

count slope 0.76296274 feet

3. Slant Range

full scale amplitude 199102 feet

count slope 6.0762963 feet

II. MLS Error Calculations

4. Azimuth Error

$$\text{AZ Error} = \text{MLS AZ} - \sin^{-1} \frac{Y(AZ)}{X(AZ)^2 + Y(AZ)^2 + Z(AZ)^2}$$

where

MLS AZ = on board recorded MLS azimuth angle

X(AZ)), Y(AZ), Z(AZ) = position of ac nose with respect
to center of azimuth array
= phototheodolite data

5. EL1 Error

$$\text{EL1 Error} = \text{MLS EL1} - \sin^{-1} \frac{Z(\text{EL1})}{\sqrt{X(\text{EL1})^2 + Y(\text{EL1})^2 + Z(\text{EL1})^2}}$$

where

MLS EL1 = on board recorded MLS EL1 angle

$$\begin{aligned} X(\text{EL1}) &= X(\text{AZ}) - \text{distance from AZ array to EL1, in feet} \\ &= Z(\text{AZ}) - 7546.8 \end{aligned}$$

$$\begin{aligned} Y(\text{EL1}) &= Y(\text{AZ}) + \text{return to runway centerline - distance} \\ &\quad \text{from centerline to EL1, in feet} \\ &= Y(\text{AZ}) + 0.88 - 254.78 \end{aligned}$$

$$\begin{aligned} Z(\text{EL1}) &= \text{height difference between AZ and EL1 antenna, in feet} \\ &= Z(\text{AZ}) - 0.47 \end{aligned}$$

6. EL2 Error

$$\text{EL2 Error} = \text{MLS EL2} - \sin^{-1} \frac{Z(\text{EL2})}{\sqrt{X(\text{EL2})^2 + Y(\text{EL2})^2 + Z(\text{EL2})^2}}$$

where

MLS EL2 = on board recorded MLS EL2 angle

$$\begin{aligned} X(\text{EL2}) &= X(\text{AZ}) - \text{distance from AZ array to EL2} + \text{distance} \\ &\quad \text{between ac nose and flare antenna, in feet} \\ &= X(\text{AZ}) - 5546.8 + 10.9 \end{aligned}$$

$$\begin{aligned} Y(\text{EL2}) &= Y(\text{AZ}) + \text{return to runway centerline - distance from} \\ &\quad \text{centerline to EL2, in feet} \\ &= Y(\text{AZ}) - 254.78 \end{aligned}$$

$$\begin{aligned} Z(\text{EL2}) &= Z(\text{AZ}) + \text{height difference between AZ and EL2} \\ &\quad \text{antenna} + \text{height difference between ac nose} \\ &\quad \text{and flare antenna, in feet} \\ &= Z(\text{AZ}) + .43 + 4 \end{aligned}$$

7. Range Error

$$\text{DME Error} = \text{DME Range} \quad X(AZ)^2 + Y(AZ)^2 + Z(AZ)^2 - 97.9$$

97.9 = DME Calibration, in feet

where

$X(AZ)$, $Y(AZ)$, $Z(AZ)$ = position of ac nose with respect to
center of azimuth array
= phototheodolite data

8. Height Error

$$\text{HT Error} = \text{MLS ABS ALT EL1} - Z(\text{GPIP})$$

where

MLS ABS ALT EL1 = height of aircraft wheels above GPIP
calculated on board from MLS EL1 and
range, in feet

$$Z(\text{GPIP}) = Z(AZ) + 11.39$$

REFERENCES

1. J. Wyatt, D. Eastman, Flight Test Demonstration of Selected Curved-Segmented Approach Paths Based on Microwave Landing System Guidance, AFFDL-TR-76-43, January 1976.
2. K. Moses, J. Doniger, T-39 Flight Guidance and Navigation System for Microwave Landing System Flight Testing, Flight Systems Division, The Bendix Corporation, AFFDL-TM-76-39, January 1976.
3. J. Wyatt, D. Eastman, ICAO Testing of a Microwave Landing System, AFFDL-TM-75-105, October 1975.
4. D. Eastman, P. Clough, Flight Test Demonstration of Automatic Landings Based on Microwave Landing System Guidance, AFFDL-TM-76-43, May 1976.

ATE
LME